DYNAMICS OF SPIN EQUILIBRIA IN METAL COMPLEXES

JAMES K. BEATTIE

School of Chemistry, The University of Sydney, New South Wales 2006, Australia

I. Introduction

Octahedral transition metal complexes with four to seven d electrons and with intermediate ligand-field strengths can exist in high-spin or low-spin electron configurations. In some cases the energies of these two configurations are sufficiently similar such that both are thermally populated at some accessible temperature. Such complexes are described as being in spin equilibrium. The interconversion between the spin states has been termed "spin-crossover." It is closely related to the intersystem crossing process in excited states. It can also be described as an intramolecular electron transfer reaction (45). Examples of octahedral spin-equilibrium complexes generally have been confined to the $3d$ transition metals, with only a few examples reported among the $4d$ elements (31, 34, 83, 142).

Four-coordinate d^8 complexes can display a closely related electronic and geometric equilibrium between paramagnetic tetrahedral and diamagnetic planar isomers. Numerous examples are known in nickel(II) chemistry (80). In this case, as well as with the octahedral complexes described above, there is no change in the coordination number of the metal ion.

A change in the spin state of a metal ion also can accompany a change in coordination number. Again, in some cases conditions may be established in which an equilibrium exists between two complexes with different coordination numbers and different numbers of unpaired electrons. Some of the concepts which are used to describe intramolecular spin equilibria can be extended to the description of these coordination-spin equilibria. Examples include equilibria among four-, five-, and six-coordinate nickel(II) complexes and equilibria involving coordination number changes in iron porphyrin complexes and in heme proteins.

The phenomenon of spin equilibrium in octahedral complexes was first reported by Cambi and co-workers in a series of papers between 1931 and 1933 describing magnetic properties of tris(N,N-dialkyldithio-carbamato)iron(III) complexes. By 1968 the concept of a thermal equilibrium between different spin states was sufficiently well established that the definitive review by Martin and White described the phenomenon in terms which have not been substantially altered subsequently (112). During the 1960s the planar–tetrahedral equilibria of nickel(II) complexes were thoroughly explored and the results were summarized in comprehensive reviews published by Holm and co-workers in 1966 and 1973 (79, 80). Also, in 1968, Busch and co-workers

published a review on iron, cobalt, and nickel complexes having anomalous magnetic moments which described, among others, complexes which undergo coordination-spin equilibria (8).

Thus 20 years ago there was an adequate understanding of many of the electronic and structural properties of complexes in spin equilibrium. There was little knowledge, however, of the dynamics of the spin equilibrium. The description of the complexes as spin isomers, with discrete nuclear configurations, and the concomitant observation of separate electronic spectra for the two spin states, set a lower limit for the spin state lifetimes longer than nuclear vibrational periods, i.e., $>10^{-13}$ second. There was some evidence that equilibration between spin states is rapid, for in certain cases averaged NMR spectra were observed in solutions, implying spin state lifetimes $<10^{-4}$ second. Furthermore, it was known that in the solid state some iron complexes display separate Mössbauer signals for the two spin isomers whereas other complexes display an averaged signal, which implies spin state lifetimes both greater than and less than the ^{57}Fe excited nuclear state lifetime of 10^{-7} second. Nevertheless, the only rate constants known had been reported from low-temperature NMR studies on the planar–tetrahedral equilibrium of dihalobis(phosphine)nickel(II) complexes (99, 129). Extrapolation to room temperature gave rate constants of the order of 10^5 sec^{-1} for the spin state interconversion.

Since 1968 there have been numerous studies on the physical and chemical properties of spin-equilibrium complexes. Many additional examples have been discovered or deliberately prepared. Extensive investigations of spin crossover in the solid state have focused on the differences between abrupt and gradual transitions which occur with a change in temperature. Most of these developments have been adequately reviewed (62, 65, 95).

This article examines the dynamics of spin-equilibrium processes, principally from studies in solutions. The properties of the complexes which are relevant to the dynamics studies are first reviewed. Then the techniques used to observe these rapid processes are described. Some aspects of solid-state dynamics are mentioned. Finally, some implications for the description of intersystem crossing processes in excited states and for spin equilibria in heme proteins are described.

Many of the complexes which occur in spin equilibrium possess ligands with complicated structures. Trivial abbreviations are used, with structural formulas given in the table in which the complex first appears. Generally the complexes are of low symmetry, but in the description of their electronic structure idealized symmetries are assumed and the appropriate term symbols are used accordingly.

II. Static Properties

A. MAGNETIC SUSCEPTIBILITY

Anomalous magnetic susceptibility is the characteristic feature of spin-equilibrium complexes. Measurement of magnetic susceptibility in the solid state, including its temperature dependence, is carried out on metal complexes using the classic Gouy and Faraday methods, as well as using the more recent techniques employing vibrating sample magnetometers and the superconducting quantum interference detector (SQUID) (121).

Measurement of magnetic susceptibility in solution is of more direct relevance to the investigation of solution dynamics. The change of state from solid to solution generally results in a change in the position of the spin equilibrium, usually but not always with an increase in the high-spin fraction. Consequently, determination of the magnetic moment in solution is desirable in order to evaluate the equilibrium constant under conditions as close as possible to those in which the dynamics are measured. Although the Gouy method can be used to measure the magnetic susceptibility of solutions, the method of choice is the nuclear magnetic resonance (NMR) technique of Evans (54).

The Evans NMR method has been widely described and applied (20, 36, 55, 87). The method involves the measurement of the chemical shift difference of the resonances of a reference molecule between a solvent and a solution containing the paramagnetic substance. An important criterion is that the reference substance does not interact directly with the paramagnetic solute. This is not a problem for most octahedral spin equilibrium complexes but must be considered in studies of coordination-spin equilibria. High-field NMR spectrometers confer advantages both of a larger intrinsic chemical shift difference due to the higher magnetic field and a twofold increase in the shift difference due to the geometry of the field parallel with instead of perpendicular to the axis of the NMR tube (15).

The Evans method gives excellent results provided adequate care is taken. A most important requirement is that the solution temperature is measured reliably. One effective means of accomplishing this for ^1H NMR is to insert into the NMR tube a capillary or additional coaxial sample of an NMR temperature calibrant solvent, usually methanol (158) or ethylene glycol (88). In this way the temperature measurement is made simultaneously with the susceptibility measurement. A second important factor is the variation of the solvent density with temperature (126). Because the density difference between the solvent and solution depends linearly on the concentration of the solute, it is only

necessary to measure the concentration dependence of the density at one temperature and to use the temperature variation of the density of the pure solvent to calculate the temperature variation of the concentration (20). A final consideration in the data analysis is the choice of the limiting moments for the high-spin and low-spin isomers. Generally the accessible temperature range is insufficient for both of these to be determined empirically. One or both moments must be treated as adjustable parameters. With judicious choices of these magnetic moments, the data give excellent linear plots of the spin-equilibrium constant with temperature (Fig. 1), from which values of ΔH^0 and ΔS^0 for the spin equilibrium can be evaluated (20). Alternatively, nonlinear behavior is an indication of more complex equilibria (61).
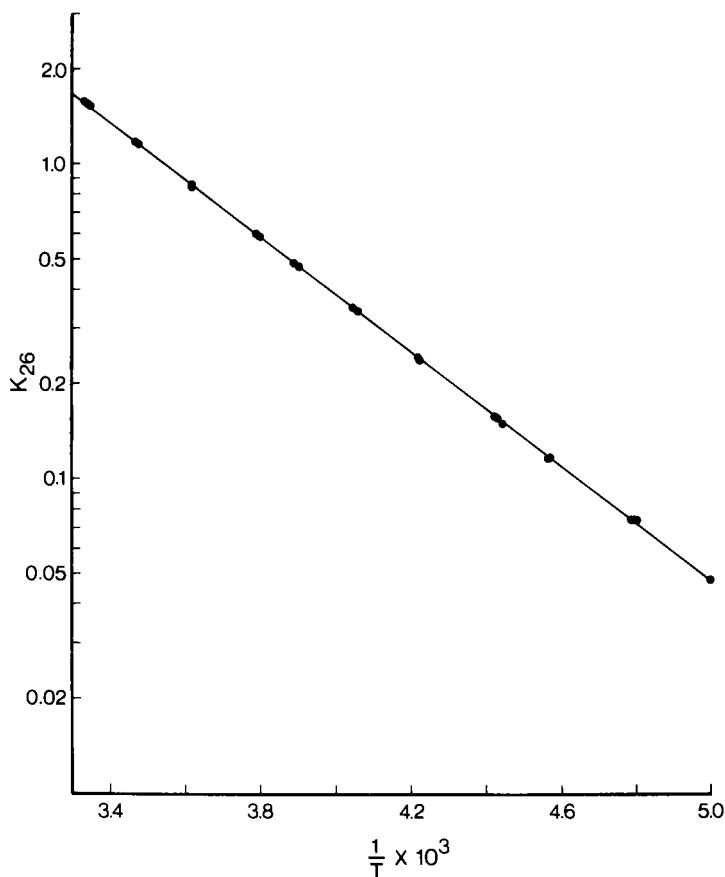

FIG. 1. Linear plot of solution magnetic susceptibility obtained by the Evans method.

Observation of magnetic susceptibility relaxation after perturbation of a spin equilibrium would be the most direct way to measure the dynamics of the equilibrium. This does not appear to have been reported as measured in solution. In principle susceptibility relaxation as a function of frequency could be measured much as dielectric relaxation is examined. The requirement is for a sufficiently strong magnetic field with very sensitive detection. A nonequilibrium magnetic susceptibility has been generated by light at low temperatures in the solid state (39).
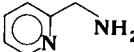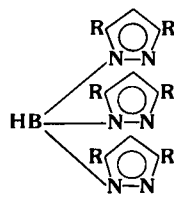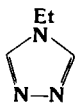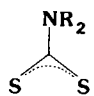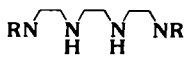
B. GEOMETRIC STRUCTURE

A change in spin state among transition metal complexes in spin equilibrium invariably involves a change in the electron population of the σ antibonding $e_g{}^*$ orbitals. This produces a substantial change in the properties of the metal–ligand bonds. This variability in the population of σ^* antibonding orbitals is a conspicuous feature of the complexes of the $3d$ transition metals and accounts for many of their unique properties.

Changes in metal–ligand bond lengths accompanying a spin state transition can be observed with X-ray crystallography in a number of ways. One is the unusual occurrence of obtaining both spin isomers in the same crystal or in closely related polymorphs. The former has been found, for example, for a dibromobis(phosphine)nickel(II) complex, with both the planar and tetrahedral isomers existing together in the same crystal (89, 92). Different spin states may also occur in crystal lattices which differ only in the degree or nature of solvation or in the identity of counterions. This has been observed, for example, in the structures of the tris(α-picolylamine)iron(II) chloride, in which the dihydrate lattice contains a low-spin complex with a facial ligand configuration, while the methanol solvate contains a high-spin complex with the meridional configuration. The difference in spin states is ascribed to differences in hydrogen bonding (64). More commonly, the two spin states are obtained by variation in temperature, although the accessible temperature range is often not wide enough to encompass the two limiting structures. Finally, comparisons can be made among closely related compounds which occur in different spin states.

Some selected data for bond length differences accompanying spin state changes are presented in Table I. For iron(II) complexes there is a substantial change of 20 pm in the iron–ligand bond length between the low-spin and high-spin states. In three cases the ligand donor atoms are all nitrogens. In another case the donor atom set is P_4Cl_2. For the four Fe^{II}–P distances the difference between the high-spin and low-spin
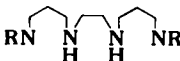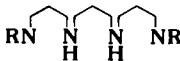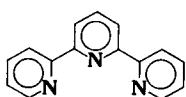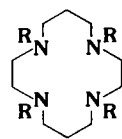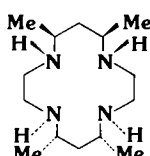
TABLE I

METAL- LIGAND BOND LENGTH DIFFERENCES BETWEEN SPIN STATES

Complex	M−L bond	Low spin (pm)	High spin (pm)	Δr (pm)	Reference
	Octahedral ⇌ Octahedral				
$[Fe(2\text{-pic})_3]Cl_2 \cdot x Sol$	$Fe^{II}-N$	201	220	19	*64, 63*
$[Fe(2\text{-pic})_3]X_2$	$Fe^{II}-N$	200	220	20	*90*

2-pic

$Fe[HB(R_2pz)_3]_2$	$Fe^{II}-N$	197	217	20	*125*

$HB(R_2pz)_3$

R= H, Me

$FeCl_2(dppen)_2 \cdot 2(CH_3)_2CO$	$Fe^{II}\;P$	230	258	28	*29*
	$Fe^{II}-Cl$	233	236	3	*29*

dppen $Ph_2PCH=CHPPh_2$

$[Fe_3(Ettrz)_6(H_2O)_6](CF_3SO_3)_6$	$Fe^{II}-N$	203	217	14	*159*

Ettrz

$Fe(dtc)_3$	$Fe^{III}-S$	230	245	15	*30*

dtc

$[Fe(R_2trien)]X$	$Fe^{III}-N$	197	214	17	*143*
	$Fe^{III}-O$	188	192	4	*143*

R_2trien

R= H$_2$Sal, acac,
acacCl,
5-OCH$_3$Sal

TABLE I (Continued)

Complex	M−L bond	Low spin (pm)	High spin (pm)	Δr (pm)	Reference
[Fe(Sal₂tet)](NO₃)	Fe^{III}−N	198	215	17	84
	Fe^{III}−O	188	194	6	84
	R₂3,2,3-tet (low spin)				
	R = Sal				
	R₂3,3,3-tet (high spin)				
	R = Sal				
[Co(terpy)₂]X₂	Co^{II}−N^a	207	214	7	58
	Co^{II}−N^b	187	208	21	58
	terpy				
Planar ⇌ Tetrahedral					
Ni(P(CH₂Ph)Ph₂)₂Br₂	Ni−P	226	231	5	92
	Ni−Br	230	235	5	92
Planar ⇌ Octahedral					
[Ni(cyclam)](ZnCl₄) ⇌ cis-[Ni(cyclam)(H₂O)₂]X₂	Ni−N	192	210	18	7
[Ni(Me₄cyclam)]X₂ ⇌ [Ni(Me₄cyclam)(H₂O)₂]X₂	Ni−N	199	214	15	9
	cyclam (R = H) Me₄cyclam (R = Me)				
[NiL$_a$](ClO₄)₂ ⇌ NiL$_a$(ClO₄)₂	Ni−N	197	207	10	75
	L$_a$				

^{a} Distal N.
^{b} Central N.

states is 28 pm, the largest observed in any octahedral spin-equilibrium complex. The difference in the Fe−Cl distances is only 3 pm, however, giving an average distance for all six ligands of 20 pm, the same as is observed for the nitrogen donor ligands. Only in the case of a complex trinuclear structure, in which just the central iron changes spin state, is the change in Fe^{II}−N distance significantly less than 20 pm.

For iron(III) complexes the differences are somewhat smaller. From a large number of structures of iron(III) dithiocarbamate complexes a difference of 15 pm can be extracted between the limiting low-spin and high-spin structures (30). From the structures of a series of hexadentate ligands derived from triethylenetetramine with N_4O_2 donor atom set, differences are found of 17 pm for the Fe−N distances, but only 4 pm for the Fe−O distances. This gives an average change in the metal−ligand distances of 13 pm.

In both the Fe(II) and Fe(III) cases the spin state change involves a change in the population of the σ antibonding $e_g{}^*$ orbitals of two d electrons. For the spin equilibrium of the d^7 cobalt(II) complexes the population of the $e_g{}^*$ orbitals changes by only one electron. From examination of the structures of a series of $[Co(terpy)_2]^{2+}$ salts, a bond length difference between the two Co−N (central) distances of 21 pm was found between the spin states, with a difference of only 7 pm found between the four Co−N (distal) distances. This gives an average difference of 12 pm.

Thus it does appear from the available evidence that the effect of the transfer of an electron from the t_{2g} to the $e_g{}^*$ orbitals is more substantial in the II oxidation state than in the III oxidation state. The $\Delta S = 1$ transition in Co(II) produces as large a bond length change as the $\Delta S = 2$ transition in Fe(III) complexes.

For nickel(II) complexes involved in planar−tetrahedral equilibria, the difference in nickel(II)−ligand distances is only 5 pm. This relatively small difference is understandable when it is recognized that the t_2 orbitals in tetrahedral complexes are only weakly σ antibonding, in contrast with the strong σ^* character of the $e_g{}^*$ orbitals in octahedral complexes. There is, of course, substantial rearrangement of bond angles.

In the planar−octahedral equilibria of nickel(II) the d orbital population changes by transfer of one electron from the $d_z{}^2$ orbital to the $d_x{}^2-y^2$ σ antibonding orbital. This results in a substantial increase in the nickel−nitrogen distances in the plane. Accompanying this is the formation of new metal−ligand bonds in the axial positions.

A change in metal−ligand distances inevitably means a change in the volume occupied by the complex, although for coordination-spin

equilibria the outcome is complicated by the different volumes occupied by the coordinated and uncoordinated ligands. For a nonzero volume change between the isomers, ΔV^0, the position of the spin equilibrium will be pressure dependent. The pressure dependence of the magnetic susceptibility has actually been measured by the Gouy method for some nickel(II) planar–tetrahedral equilibria (53), and for the spin equilibria of some iron(III) dithiocarbamate complexes (52). The Evans NMR method does not yet appear to have been used under high pressure to obtain ΔV^0 for spin equilibria, but with the increasing availability of high-pressure NMR techniques (47) this method will surely be used for this purpose.
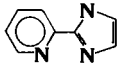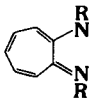
The pressure dependence of other properties can be used to calculate ΔV^0. Because the volume differences between the spin states are relatively large, pressures of up to only 1000–3000 atm are sufficient to cause a significant shift in the spin equilibrium. Observation of the change in the electronic absorption spectrum, for example, enables calculation of ΔV^0, with the help of certain assumptions and ancillary experiments (19). The extinction coefficients for absorption by the two isomers must be obtained. In the simplest model they are assumed to be independent of pressure. In one approach (19) they were found by examination of the temperature dependence of the electronic absorption spectrum. This required knowledge of the temperature dependence of the spin-equilibrium constant, which was obtained from the temperature dependence of the susceptibility observed in the Evans NMR experiment. Clearly a more direct measurement is preferable.

The pressure dependence of the NMR spectrum of a nickel(II) complex which undergoes a coordination-spin equilibrium has been used to obtain the volume difference between the planar and octahedral isomers (118). In this case both the temperature and pressure dependence of the NMR spectra were analyzed simultaneously to yield five parameters, ΔH^0, ΔS^0, ΔV^0, and the chemical shifts of the two isomers. Subsequent determinations from the electronic spectra and ultrasonics relaxation are in good agreement with the NMR result (13).

The volume difference can be found without the use of high-pressure techniques in favorable cases from the amplitude of the sound absorption observed in ultrasonic relaxation of the spin equilibrium. This method will be described below in Section III,C.

Values of ΔV^0 obtained for a number of different spin equilibria by a variety of techniques are presented in Table II. Volumes of activation, ΔV^*, obtained from the pressure dependence of the rates of spin state interconversion, will be described in Section IV,A.

TABLE II

Volume Differences, ΔV^0, between Spin States

Complex	Method[a]	ΔV^0 (cm³ mol⁻¹)	Reference
Octahedral ⇌ Octahedral			
Fe^{II}(HB(pz)$_3$)$_2$	U	23.6	12
[Fe(pyim)$_3$]$^{2+}$	E	14.3[b]	115
	E	10.3[c]	115
	E	5.3[d]	115
pyim			
[Fe(bzim)$_3$]$^{2+}$	E	12.4[b]	115
	E	9.6[c]	115
	E	4.3[d]	115
Fe^{III}(dtc)$_3$[e]	G	4–6	52
[Fe^{III}(acac)$_2$trien]$^+$	U	10.3	22
[Fe^{III}(sal)$_2$trien]$^+$	U	11.9	22
[Co^{II}(terpy)$_2$]$^{2+}$	E	10.1	18
Planar ⇌ Tetrahedral			
Ni(ethyl-ati)$_2$	G	7.5	53
Ni(n-propyl-ati)$_2$	G	8	53
Ni(β-naphthyl-ati)$_2$	G	8.5[f]	53
	G	5[g]	53
Ni(p-anisidyl-ati)$_2$	G	7.5[f]	53
	G	~4[g]	53
R-ati			

R= Et,
n-propyl,
β-Naphthyl,
p-Anisidyl

Complex	Method[a]	ΔV^0 (cm³ mol⁻¹)	Reference
Planar ⇌ Octahedral			
[Ni(Me$_4$cyclam)]$^{2+}$/(H$_2$O)$_2$	U	−10.1	13
	E	−8.6	13
	N	−10.0	118
[Ni(cyclam)]$^{2+}$/(H$_2$O)$_2$	E	−3.5	13
[Ni(2,3,2-tet)]$^{2+}$/(H$_2$O)$_2$	N	−3	123

[a] Methods: E, electronic spectra; G, Gouy; N, NMR; U, ultrasonic relaxation.
[b] CH$_3$CN.
[c] Acetone.
[d] CH$_3$OH plus 20% CH$_3$CN.
[e] A large number of complexes measured in different solvents.
[f] CHCl$_3$ solution.
[g] CH$_2$Cl$_2$ solution.

C. Electronic Spectra

The existence of spin states with significantly different metal–ligand bond lengths requires the isomers to exist with distinctly different electronic structures and properties. The spin-pairing energy for $3d$ electrons in a transition metal complex is of the order of 10,000–20,000 cm^{-1} (94). A useful illustration of this energy is the spectrum of chromium(III) complexes, in which the $^4A \rightleftarrows {}^2E$ transition corresponds to spin pairing from a quartet $(t_{2g})^3$ to a doublet $(t_{2g})^3$ d electron configuration. The transition occurs without any change in the e_g^* antibonding population and produces accordingly a sharp spin-forbidden electronic band, exploited in the ruby laser. Its energy is about 16,000 cm^{-1}.

To compensate for this endothermic spin-pairing energy in the transition from the weak-field high-spin to the strong-field low-spin state, there is a substantial increase in the ligand-field stabilization energy. This arises from a significant increase in the ligand-field strength due to the shorter, stronger metal–ligand bonds. König and co-workers have evaluated Δ for the high-spin and low-spin states of [Fe(phen)$_2$(NCS)$_2$] to be 11,900 and 16,300 cm^{-1}, respectively (93). They subsequently measured an average metal–ligand bond length difference of 12 pm between the spin states, and observed that this is precisely what is predicted by ligand-field theory in which Δ depends inversely on the fifth power of the metal–ligand distance (96).

From these considerations it is clear that complexes in spin equilibrium do not exist at the crossover point between high-spin and low-spin configurations represented on a Tanabe–Sugano diagram. The two states are electronic isomers with geometric and electronic structures well separated on either side of the crossover point. The energy required to reach the crossover point represents at least part of the activation energy for the spin state interconversion.

Thus the electronic structure of each spin state leads to a distinctive electronic absorption spectrum for that state. The observed spectrum is the superposition of the spectra of the two isomers with different ligand fields. Interconversion is slow on the electronic time scale. There is no dynamic information in the spectrum but it can be used as a probe of the concentrations of the two spin states.

This description is most appropriate for those $\Delta S = 2$ spin equilibria of octahedral Fe(II) and Fe(III) in which spin-orbit coupling does not directly mix the two spin states. It is possibly less appropriate for $\Delta S = 1$ transitions for which sufficiently strong mixing could lead to a quantum mechanically mixed spin state as the ground state. That is, instead of two potential wells there is could be a single minimum (3, 6). There is

little evidence for this phenomenon in octahedral complexes, but it has been described in five-coordinate complexes (*160*) and in tetragonally distorted complexes formed by porphryins and hemes. The latter will be discussed in Section VII,B.

There have been some measurements of the X-ray photoelectron spectra of spin-equilibrium complexes. Considerable difficulties have been encountered from X-ray-induced sample decomposition. Binding energy differences of a few tenths of an electron volt have been observed (*24, 103, 156*).

D. VIBRATIONAL SPECTRA

The description of spin states as electronic isomers with different metal–ligand distances requires that their vibrational spectra be a superposition of the spectra of the two separate spin states. The relative contribution of the two states to the observed spectrum will change with temperature as the population of the spin states changes. This has been observed (*76, 77, 122, 144, 145*). Difficulties occur with the assignment of the metal–ligand vibrational frequencies of particular interest for the analysis of the dynamics of spin state transitions. Some success has been achieved with the use of metal isotopic labeling (*82, 151*), but there are few reliable assignments.

The significance of these results is the demonstration that separate spin isomers do exist with distinctive vibrational spectra. Large differences have been observed, for example, in metal-sensitive infrared frequencies of $[Fe^{II}(pz)_3)_2]$. The low-spin isomer possesses metal–ligand bands in the region 450-400 cm^{-1} while the high-spin isomer has bands in the region 250–200 cm^{-1} (*82*). This is consistent with the 20-pm lengthening of the iron(II)–nitrogen bond which accompanies the spin state change (*125*).

There have been very few reports of the Raman spectra of spin-equilibrium complexes. In one experiment the presence of both high-spin and low-spin isomers of an iron(II) Schiff base complex was observed by the resonance Raman spectra of the imine region (*11*). The temperature dependence of the spectra was recorded for both solid and solution samples. Recently differences were described in the resonance Raman spectra of four- and six-coordinate nickel(II) porphyrin complexes which undergo coordination-spin equilibria. These studies are extensions of a considerable literature on spin state effects on the Raman spectra of iron porphyrins and hemes. There are apparently no reports of attempts to use time-resolved Raman spectra for dynamics experiments.
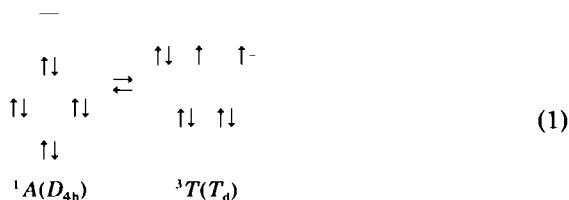
III. Techniques

The rapidity of spin state interconversions requires that relaxation methods be used to investigate spin equilibrium dynamics in solution. Only in the case of coordination-spin equilibria might the addition of low concentrations of ligands be observable by rapid mixing techniques with a high sensitivity detection method. In addition, the temperature coefficients of the rate constants are usually relatively small, so that lowering the temperature does not produce a large reduction in the rates. Consequently, the dynamics of spin state equilibria has generally been investigated with microsecond to nanosecond relaxation methods.

A. MAGNETIC RESONANCE METHODS

In principle magnetic resonance methods are ideally suited to monitor the dynamics of spin equilibria. A spin crossover by definition produces a change in the number of unpaired electrons and hence in the magnetic moment of the complex. This necessarily affects the magnetic resonance spectra of the complex. Extensive use has been made of the resulting large paramagnetic chemical shifts for the purpose of determining the equilibrium constants and temperature dependence of spin equilibria (*69, 80, 86*).

NMR has not proved generally useful, however, for examining the dynamics of spin equilibria. Low-temperature proton NMR has been used successfully to obtain rates for some planar–tetrahedral equilibria in nickel(II) complexes (*99, 129, 130, 134*). Equation (1) illustrates the orbital occupancy and ground state terms for the d^8 equilibrium:

$$
\begin{array}{ccc}
\overline{\quad} & & \uparrow\downarrow \;\; \uparrow \;\; \uparrow\text{-} \\
\uparrow\downarrow & \rightleftarrows & \\
\uparrow\downarrow \quad \uparrow\downarrow & & \uparrow\downarrow \;\; \uparrow\downarrow \\
\uparrow\downarrow & & \\
{}^1A(D_{4h}) & & {}^3T(T_d)
\end{array}
\tag{1}
$$

In this case the planar complex is diamagnetic and possesses the usual narrow line, high-resolution diamagnetic spectrum. The tetrahedral complex in T_d symmetry would possess a ^3T ground state. In approximately tetrahedral nickel(II) complexes the orbital angular momentum is incompletely quenched; the result is a very short electron spin relaxation time and an NMR spectrum with relatively narrow, paramagnetic shifted resonances.

The effect of interconversion between the planar and tetrahedral isomers on the NMR spectrum can be described by extension of the analysis for exchange between two diamagnetic sites (*149*). It should be noted that the well-known analysis of Swift and Connick (*146, 148*) is not directly applicable, because the paramagnetic site is not dilute, as it is in the case of solvent exchange on a paramagnetic metal ion.

Care must be taken to identify properly the exchange regime being observed. Only under slow exchange conditions can the exchange lifetime be extracted directly from the linewidth; otherwise the system must be analyzed to determine the chemical shift difference between the two sites and the relaxation time of the paramagnetic resonance. This identification is usually made from the temperature dependence of the observed linewidth. This procedure is complicated for spin equilibria by the temperature dependence of the mole fraction of the paramagnetic species as well as by the Curie temperature dependence of its paramagnetism. The dynamic properties of the spin equilibrium are superimposed on its anomalous magnetic properties. Despite these difficulties rate constants have been extracted.

For octahedral complexes only in the d^6 case does equilibrium occur between a diamagnetic state and a paramagnetic T state. In the other three cases one of the isomers is in a paramagnetic A or E ground state [Eqs. (2–5)].

$$
\begin{array}{cccccc}
- & - & & \uparrow & - & \\
\uparrow\downarrow & \uparrow & \uparrow\text{-} & \rightleftarrows & \uparrow\text{-} & \uparrow & \uparrow \\
& {}^3T & & & {}^5E &
\end{array}
\tag{2}
$$

$$
\begin{array}{cccccc}
- & - & & \uparrow & \uparrow & \\
\uparrow\downarrow & \uparrow\downarrow & \uparrow & \rightleftarrows & \uparrow\text{-} & \uparrow & \uparrow\text{-} \\
& {}^2T & & & {}^6A &
\end{array}
\tag{3}
$$

$$
\begin{array}{cccccc}
- & - & & \uparrow & \uparrow & \\
\uparrow\downarrow & \uparrow\downarrow & \uparrow\downarrow & \rightleftarrows & \uparrow\downarrow & \uparrow\text{-} & \uparrow \\
& {}^1A & & & {}^5T &
\end{array}
\tag{4}
$$

$$
\begin{array}{cccccc}
\uparrow & - & & \uparrow\text{-} & \uparrow\text{-} & \\
\uparrow\downarrow & \uparrow\downarrow & \uparrow\downarrow & \rightleftarrows & \uparrow\downarrow & \uparrow\downarrow & \uparrow \\
& {}^2E & & & {}^4T &
\end{array}
\tag{5}
$$
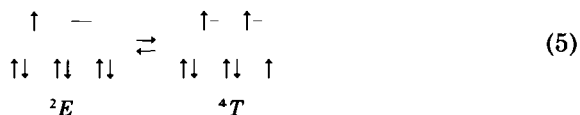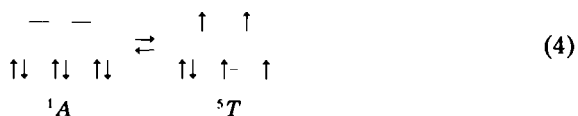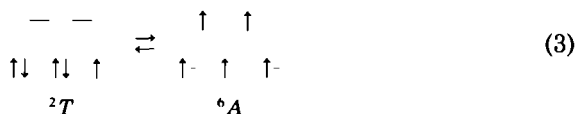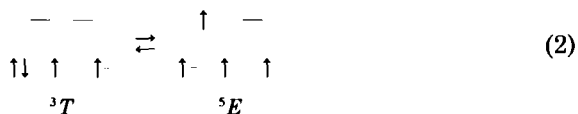
These A and E states have long electron relaxation times which generally result in broad, unobservable NMR spectra. Hence it would

be difficult to identify properly the exchange regime, even if dynamic effects were apparent in the NMR spectrum. In fact, where NMR spectra have been recorded, only exchange-averaged spectra are observed. This apparently arises because the spin equilibrium is established rapidly compared with the chemical shift difference between the spin states or the paramagnetic relaxation time, T_{2m}. Possibly even higher magnetic fields or more sophisticated pulse experiments could be used to address the problem.

Because NMR has in general been too slow a technique to observe the dynamics of octahedral spin equilibria, the higher frequency of observation of electron paramagnetic resonance (EPR) would seem well suited to this purpose. Despite the inevitable presence of unpaired electrons on complexes in spin equilibrium, there are serious limitations on the use of EPR, which are complementary to those of NMR. Diamagnetic states do not possess an EPR spectrum. Paramagnetic states with orbital angular momentum (T states) generally have a very short electron spin relaxation time, which leads to a broad EPR spectrum that is difficult to observe except at very low temperatures. In one novel attempt to circumvent this limitation, Mn(II) was doped into a lattice of an iron(II) spin-equilibrium complex and used as a probe of the magnetism (136). In general, however, only d^4 and d^7 octahedral complexes with paramagnetic E states are promising candidates for EPR experiments. While some signals have been observed for spin equilibrium complexes and can be used to place limits on the rates of spin state interconversion, the technique has not been widely applied.

B. TEMPERATURE-JUMP RELAXATION

All intramolecular spin equilibria have a nonzero enthalpy of reaction. This occurs because the high-spin isomer possesses greater entropy, both from its higher spin degeneracy and from its larger vibrational partition function, than does the low-spin isomer. Because ΔG is approximately zero, ΔH is therefore positive. Consequently, the equilibria are temperature dependent and can be perturbed by a rapid change in temperature.

The Joule heating temperature-jump experiment involves the discharge of a high voltage through a conducting solution to produce a temperature rise of a few degrees in several microseconds (59, 72). For nonconducting solutions microwave heating has been used, again with a heating rise time of some microseconds (25). Both of these techniques have been used to investigate coordination-spin equilibria, but have proved too slow to observe most intramolecular spin equilibria.

A major advance in the investigation of the intramolecular dynamics of spin equilibria was the development of the Raman laser temperature-jump technique (43). This uses the power of a laser to heat a solution within the time of the laser pulse width. If the relaxation time of the spin equilibrium is longer than this pulse width the dynamics of the equilibrium can be observed spectroscopically. At the time of its development only two lasers had sufficient power to cause an adequate temperature rise, the ruby laser at 694 nm and the neodymium laser at 1060 nm. Neither of these wavelengths is absorbed by solvents. Various methods were used in attempts to absorb the laser power, with partial success for microsecond relaxation times.

Nanosecond observations became possible with application of the stimulated Raman effect (16, 157). A schematic diagram of the experiment is shown in Fig. 2. Up to 10% of the power of the laser pulse can be scattered in the forward direction at a longer wavelength, which is the incident wavelength less the Raman energy of the scattering medium. With liquid N_2 as the Raman absorber, the energy of the Nd laser is shifted by the N–N Raman stretching frequency to 1410 nm (1.41 μm, 7090 cm^{-1}). This is the frequency of the first overtone of the O–H stretching frequency of water. Because the energy is absorbed in a vibrational mode of the solvent, and vibrational–translational energy transfer occurs within picoseconds, the temperature rise occurs within the time of the laser pulse width. The laser pulse triggers observation of the relaxation dynamics, which is typically performed spectrophotometrically with an interrogating beam focused on the heated volume of solvent and detected with single-shot transient recording. A few tenths of a millimeter thickness of water or other hydroxylic solvents can be heated several degrees within 20 nsec with this technique. High-pressure hydrogen can also be used as the Raman scatterer to shift the Nd laser energy to 1.89 μm (5290 cm^{-1}) which is absorbed by a number of nonaqueous solvents (2).
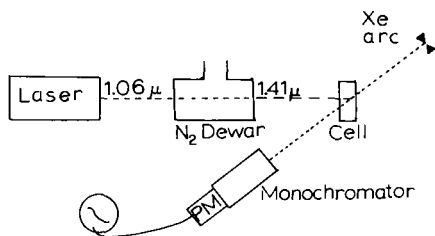

FIG. 2. Schematic diagram of the Raman laser temperature-jump experiment.

The Raman laser temperature-jump technique has been used in studies of a variety of spin-equilibrium processes. It was used in the first experiment to measure the relaxation time of an octahedral spin-equilibrium complex in solution (14). Its applications include investigations of cobalt(II), iron(II), iron(III), and nickel(II) equilibria.

C. ULTRASONIC RELAXATION

Spin equilibria are pressure dependent because the change in metal–ligand distances that accompanies the spin state transition produces a change in the volume of the complex. The single-step pressure-jump relaxation technique has an observation time of the order of 10^{-4} second, which is too slow to observe spin-equilibria dynamics. The periodic pressure variation of a sound wave, however, can be used for this purpose. Two different ultrasonic techniques have been used—the resonator method and the pulse method (50, 147). These span different frequency ranges. The resonator method operates from below 1 to above 15 MHz, or from 6×10^6 to 10^8 radians sec^{-1}, corresponding to relaxation times from longer than 10^{-7} to 10^{-8} second. The pulse method operates conveniently in the range 15–150 MHz, corresponding to relaxation times from 10^{-8} to 10^{-9} second.

Perturbation of a chemical equilibrium by ultrasound results in absorption of the sound. Ultrasonic methods determine the absorption coefficient, α (neper cm^{-1}), as a function of frequency. In the absence of chemical relaxation the background absorption, B, increases with the square of the frequency f (hertz); that is, α/f^2 is constant. For a single relaxation process the absorption increases with decreasing frequency, passing through an inflection point at the frequency ω (radians $sec^{-1} = 2\pi f$) which is the inverse of the relaxation time, τ (seconds), of the chemical equilibrium [Eq. (6) and Fig. 3].

$$\alpha/f^2 = A(1 + \omega^2\tau^2)^{-1} + B \qquad (6)$$

The absorption due to the chemical relaxation, A, is obtained from the low-frequency absorption where $\omega \ll \tau$ [Eq. (7)].

$$A = \frac{2\pi^2\rho v}{RT}\left[\Delta V^0 - \frac{\alpha_\mathrm{p}}{\rho C_\mathrm{p}}\Delta H^0\right]^2 \Gamma\tau \qquad (7)$$

In Eq. (7) ρ is the solution density, v is the sound velocity, α_p is the coefficient of thermal expansion, C_p is the specific heat, and Γ is the concentration dependence of the equilibrium. Neglecting activity
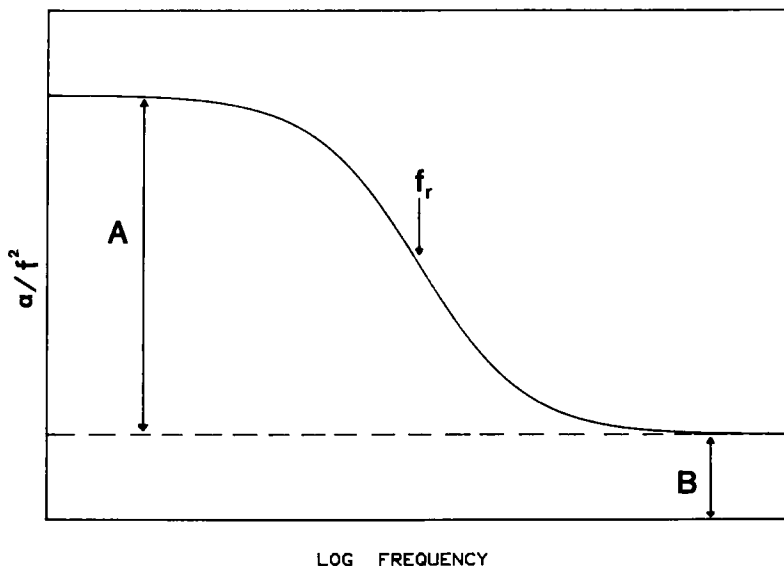
FIG. 3. Ultrasonic absorption curve for a single relaxation process.

coefficients, $\Gamma^{-1} = \sum_i \nu_i^2/c_i$, where ν_i is the stoichiometric coefficient of the ith species and c_i its concentration. For a unimolecular spin equilibrium, $\Gamma^{-1} = [LS]^{-1} + [HS]^{-1}$, where [LS] and [HS] are the concentrations of the low-spin and high-spin species, respectively. Thus the ultrasonic relaxation absorption amplitude is a maximum when both spin isomers are present in equal concentrations.

Measurement of an ultrasonic relaxation curve enables evaluation of both the relaxation time, τ, and the relaxation amplitude, A. Interpretation of the relaxation time requires knowledge of the equilibrium constant. For a intramolecular isomerization such as a high-spin $\rightleftarrows$ low-spin equilibrium, the forward and reverse rate constants, k_1 and k_{-1}, respectively, can be evaluated from the relaxation time and the equilibrium constant from Eq. (8) (17).

$$\tau^{-1} = k_1 + k_{-1} = k_{-1}(K + 1) \tag{8}$$

From the amplitude of the low-frequency excess sound absorption, A, the volume difference between the two isomers can be evaluated. This again requires knowledge of the equilibrium constant, in order to evaluate Γ, of the relaxation time τ, and of the standard enthalpy
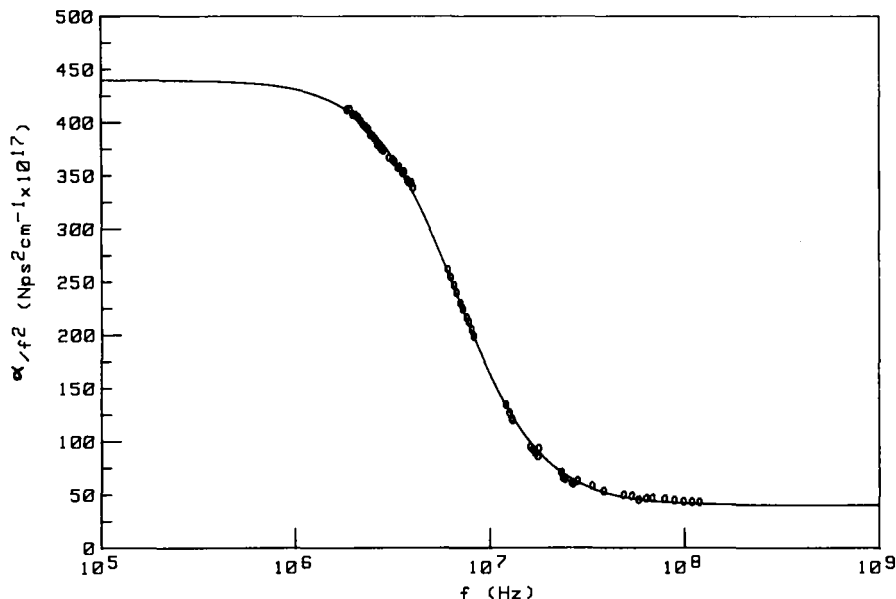
FIG. 4. Ultrasonic absorption data for an intramolecular spin-equilibrium relaxation.

change, ΔH^0. Consequently, a thorough investigation of the static equilibrium properties of the isomerization is required before the ultrasonics data can be fully evaluated. This is necessary in any case because it is necessary to have some independent evidence in order to assign confidently an observed ultrasonic absorption to a particular dynamic process. When this has been achieved, data of high precision can be obtained (Fig. 4).

D. PHOTOPERTURBATION

It is possible to perturb a spin equilibrium by photoexciting one of the isomers. Among the possible radiative and nonradiative fates of the excited state is intersystem crossing to the manifold of the other spin state. Internal conversion within this manifold ultimately results in the nonequilibrium population of the ground state. If these processes are rapid compared with the relaxation time of the spin equilibrium, then the dynamics of the ground state spin equilibrium can be observed. This experiment was first performed for spin equilibria with a coordination-spin equilibrium of a nickel(II) complex (85). More recently a similar phenomenon has been observed in the solid state at low temperatures (41). The nonequilibrium distribution can be trapped for long periods at

sufficiently low temperatures; the effect has been termed "light-induced excited spin state trapping" (LIESST).

A question immediately arises whether the observed relaxation is that of the ground state or of some photochemical or photophysical process of the excited states. For the particular nickel(II) complex first studied in solution the relaxation was positively identified as the relaxation of the ground state equilibrium in an elegant experiment by Creutz and Sutin (37). Photoexcitation with the 1.06-μm radiation of a neodymium laser pulse results in depopulation of the octahedral complex. The subsequent reestablishment of the equilibrium is observed as a decrease in the absorbance of the planar complex, with a relaxation time of 0.30 $\pm$ 0.02 μsec. By Raman shifting the laser output to 1.41 μm the experiment is converted into a temperature-jump relaxation. Because ΔH^0 is negative for the planar-to-octahedral equilibrium, the increase in temperature results in an increase in the absorbance by the planar complex, again with the same relaxation time of 0.30 $\pm$ 0.02 μsec. This demonstrates that the photoexcitation does result in perturbation of the ground state equilibrium. An alternative means of establishing this is to scan the spectrum of the perturbed equilibrium to ascertain whether it corresponds to the ground state species.

This photoperturbation technique has been applied to a number of different spin-equilibrium complexes. Its success is apparently due to the fact that the relaxation times of the spin equilibria are longer in each case than the radiative and nonradiative processes in the excited states.

E. Mössbauer Spectroscopy

Mössbauer spectroscopy of the ^{57}Fe nucleus has been extensively used to investigate aspects of spin equilibria in the solid state and in frozen solutions. A rigid medium is of course required in order to achieve the Mössbauer effect. The dynamics of spin equilibria can be investigated by the Mössbauer experiment because the lifetime of the excited state of the ^{57}Fe nucleus which is involved in the emission and absorption of the γ radiation is 1×10^{-7} second. This is just of the order of the lifetimes of the spin states of iron complexes involved in spin equilibria. Furthermore, the Mössbauer spectra of high-spin and low-spin complexes are characterized by different isomer shifts and quadrupole coupling constants. Consequently, the Mössbauer spectrum can be used to classify the dynamic properties of a spin-equilibrium iron complex.

If the interconversion between the spin states is slow on the Mössbauer time scale, that is $\tau \gg 10^{-7}$ second, then the observed spectrum comprises the superposition of the spectra of the two separate spin states. This has been the most common observation. The areas of the two superimposed spectra can be used to estimate the relative populations of the two spin states. Their change with temperature can be used to ascertain whether the spin transition in the solid state is abrupt or gradual. These questions have been intensively investigated and reviewed (*35, 66–68*).

If the spin state interconversion is faster than the excited nuclear state lifetime, that is $\tau \ll 10^{-7}$ second, then the observed spectrum is an average of the spectra of the two spin states. Until recently this condition had been observed only for iron(III) complexes with thiocarbamate or selenocarbamate ligands—ferric dithiocarbamates (*119*), monothiocarbamates (*98*), or diselenocarbamates (*42*). Since 1982, however, there have been a number of reports of other iron(III) complexes which also display an averaged Mössbauer spectrum (*56, 57, 108–111, 124, 153, 155*).

If some iron(III) complexes undergo rapid spin interconversion on the Mössbauer time scale, and some undergo slow interconversion, then it is inevitable that a few will interconvert, at some accessible temperature, at a rate which produces dynamic effects on the Mössbauer spectrum. Such examples have now been found (*109, 111*). Rate constants have been extracted from these spectra and are necessarily of the order of $10^6 – 10^7 \sec^{-1}$. The interpretation of the spectral lineshapes is complex (*153, 154*), however, and further work will be needed to establish the reliability of the rate data obtained from such spectra.

IV. Solution Dynamics
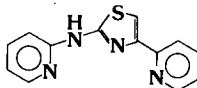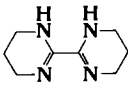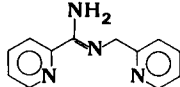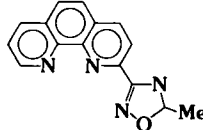
A. IRON(II)

The dynamics of an octahedral spin equilibrium in solution was first reported in 1973 for an iron(II) complex with the Raman laser temperature-jump technique (*14*). A relaxation time of 32 ± 10 nsec was observed. Subsequently, further studies have been reported with the use of this technique, with ultrasonic relaxation, and with photoperturbation. Selected results are presented in Table III.

One striking feature of these results is the narrow range of relaxation times represented; they span only a range of four from 30 to 120 nsec. In part, this is an artifact of the relaxation techniques used, and in part, it

TABLE III

DYNAMICS OF $^1A \rightleftarrows {}^5T$ EQUILIBRIA OF IRON(II) COMPLEXES IN SOLUTION AT OR NEAR 298 K

Complex	Solvent	Method[a]	τ (nsec)	k_{15} (sec^{-1})	Reference
Fe(HB(pz)$_3$)$_2$	CH$_2$Cl$_2$/CH$_3$OH	T	32 ± 10	1×10^7	14
	THF	U	33.0 ± 0.7	4.9×10^6	12
Fe(6-MePy)(Py)$_2$tren^{2+}	CH$_3$OH; acetone/H$_2$O	T	120 ± 20	4×10^5	81
Fe(6-MePy)$_2$(Py)tren^{2+}	Acetone/H$_2$O; CH$_3$OH/H$_2$O	T	110 ± 30	4×10^6	81

$$RR'R''\text{tren} \quad N\left(CH_2CH_2N=C \overset{H}{\underset{N}{}} R,R',R''\right)_3$$

R,R'= 6-MePy; R''= Py or
R = 6-MePy; R',R''= Py

Fe(papth)$_2^{2+}$	H$_2$O	U	41.0 ± 0.2	1.7×10^7	12

papth

Fe(pyim)$_3^{2+}$	CH$_3$CN/CH$_3$OH	T	48 ± 8	1.1×10^7	137
	CH$_3$CN/CH$_3$OH	P	50 ± 3		114
	Acetone	P	45 ± 5		44
Fe(biz)$_3^{2+}$	CH$_3$CN	P	27		114

biz

Fe(ppa)$_2^{2+}$	H$_2$O	P	102		114

ppa

Fe(phenmethoxa)$_2^{2+}$	Acetone	P	110 ± 10	7.7×10^6	44

phenmethoxa

[a] Methods: T, Raman laser temperature-jump; U, ultrasonic relaxation; P, photoperturbation.

is a feature of the complexes that can be studied, as will be discussed below. The rate constants span a wider range, from 10^5 to 10^7 sec^{-1}, which reflects the range of the spin-equilibrium constants.

A second feature is the good agreement between the relaxation times observed using different techniques. After the first relatively imprecise study of $Fe(HB(pz)_3)_2$ with the Raman laser temperature-jump technique, the equilibrium was reinvestigated using the more precise ultrasonic relaxation method. Excellent agreement was found between the two methods. Similarly, the relaxation of the spin equilibrium in $Fe(pyim)_3^{2+}$ has been investigated in three different laboratories; two used the photoperturbation method and one the temperature-jump method. All three results were identical within experimental error. This is a particularly important observation, because of the uncertainty concerning the consequences of photoexcitation. For both the iron(II) complex described here and a nickel(II) complex described elsewhere, however, photoexcitation has been shown to result in perturbation of the spin equilibrium, which implies that the excited states decay rapidly and that at least some decay to the other isomer, perturbing the spin equilibrium.

Another feature of these results is that the relaxation time appears to be nearly solvent independent, in those cases in which studies have been performed in different solvents. This indicates that the dynamics of the spin equilibrium is predominately determined by intramolecular properties. There are some complexes for which hydrogen bonding to the solvent plays a significant role and both reaction volumes and activation volumes have been observed to be solvent dependent (115).

Consideration of the thermodynamics of a representative reaction coordinate reveals a number of interesting aspects of the equilibrium (Fig. 5). Because the complex is in spin equilibrium, $\Delta G^0 \approx 0$. Only complexes which fulfill this condition can be studied by the Raman laser temperature-jump or ultrasonic relaxation methods, because these methods require perturbation of an equilibrium with appreciable concentrations of both species present. The photoperturbation technique does not suffer from this limitation and can be used to examine complexes with a larger driving force, i.e., $\Delta G^0 \ll 0$. In such cases, however, ΔG^0 is difficult to measure and will generally be unknown.

For those systems with $\Delta G^0 \approx 0$, it follows that $\Delta H^0 \approx T\Delta S^0$. Conversion from the low-spin to the high-spin state involves lengthening and weakening the metal–ligand bonds. This results in a high-spin state with higher enthalpy and also greater entropy. Such a reaction profile is shown in Fig. 5 for the $Fe(HB(pz)_3)_2$ complex.

The activation parameters indicate that the quintet–singlet process,

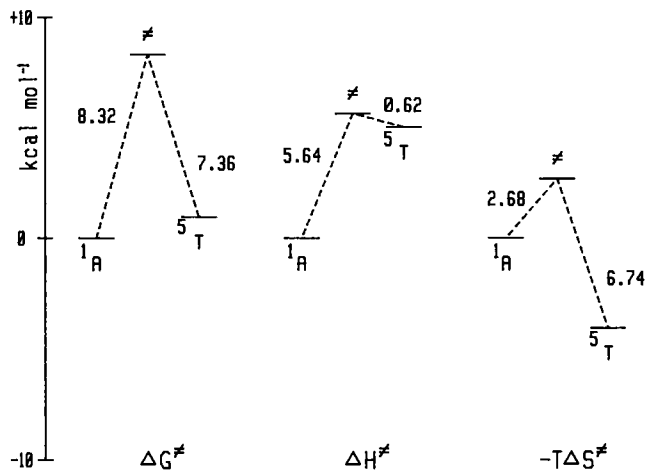FIG. 5. Reaction coordinate profile for the octahedral spin equilibrium of [Fe(HB(pz)$_3$)$_2$].

represented by rate constant k_{51}, proceeds with a very small enthalpic barrier. This allows some inferences about the adiabaticity of the spin-forbidden transition. In conventional transition state theory the transmission coefficient, κ, is assumed to be unity.

$$k = \kappa(k_B T/h)\exp(-\Delta G^*/RT) \qquad (9)$$

For these spin-forbidden transitions, with $\Delta S = 2$, this assumption is very likely invalid and the process is nonadiabatic, i.e., $\kappa < 1$. If it is assumed that the entire entropic barrier of the quintet–singlet transition is due to nonadiabaticity, a minimum value of $\kappa \sim 10^{-4}$ is obtained.

The assumption that the entropic barrier to the spin state transition is due entirely to spin-forbidden nonadiabaticity is equivalent to assuming that the transition state has the structure of the high-spin state. This is unlikely to be the case, and insofar as the assumption is invalid, the minimum value of κ is increased. There is some evidence from the volume of activation for the spin state transition that the transition state lies well along the reaction coordinate between the low-spin and high-spin states. This novel experiment was accomplished independently by two groups with use of the photoperturbation technique with the sample subjected to variable pressure (44, 115). In the two cases reported, the volume of activation places the transition state about midway between the low-spin and high-spin states. If this is correct then there will be a considerable "chemical" contribution to the

entropy of activation, due to the change in the structure and vibrational properties of the complex. The estimated minimum value of the transmission coefficient, κ, is correspondingly larger and the reaction process is correspondingly less "spin-forbidden." The available evidence would suggest that κ is no smaller than the order of 10^{-2}.

B. IRON(III)

The spin-equilibrium dynamics of iron(III) complexes in solution have been examined with the techniques of Raman laser temperature-jump, ultrasonic relaxation, and photoperturbation. The complexes investigated, the relaxation times observed, and one of the derived rate constants are presented in Table IV. Many of the relaxation times are quite short, and some of the original temperature-jump results ([45]) were found to be inconsistent with more accurate ultrasonic experiments ([20]) and later photoperturbation experiments ([102]). It has not been possible to repeat some of these laser temperature-jump observations. Instead, the expected absorbance changes and isosbestic points were found to occur within the heating rise time of the laser pulse, consistent with the ultrasonic and photoperturbation experiments ([20]). Consequently, none of the original Raman laser temperature-jump results is included in Table IV.

A number of observations indicate interconversion rates for some iron(III) complexes too fast to measure with existing techniques. Relaxation times less than the 30-nsec limit set by the heating rise time of the laser temperature-jump technique were observed for [Fe(benzac$_2$trien)]$^+$, [Fe(Salmeen)$_2$]$^+$, and [Fe(Me$_2$dtc)$_3$] ([45, 128]). From ultrasonic observations a limit of less than 1 nsec was placed on the relaxation time for the first of these compounds,

TABLE IV

DYNAMICS OF $^2T \rightleftarrows {}^6T$ EQUILIBRIA OF IRON(III) COMPLEXES IN SOLUTION AT 298 K

Complex[a]	Solvent	Method[b]	τ (nsec)	k_{26} (sec^{-1})	Referen
Fe(Sal$_2$trien)$^+$	H$_2$O	U	5.33(5)	6.1×10^7	21, 20
	CH$_3$OH	P	5(1)	6.1×10^7	102
	Acetone	P	3(1)	6.1×10^7	102
Fe(acac$_2$trien)$^+$	H$_2$O	U	2.11(4)	1.6×10^8	20
Fe(5-OCH$_3$Sal$_2$trien)$^+$	Acetone/CH$_3$OH	P	5(1)	—	102

[a] For ligand abbreviations, see Table II.
[b] Methods: U, ultrasonic relaxation; P, photoperturbation.

[Fe(benzac$_2$trien)]$^+$ (20). These observations, together with the short relaxation times presented in Table IV, indicate that spin state interconversions in iron(III) complexes are slightly more rapid than those observed in iron(II) complexes. There are only a limited number of results available at present, however, and these may not be representative.

C. COBALT(II)

The cobalt(II) complexes which undergo spin equilibrium are of several different types. Octahedral high-spin complexes with a ^4T ground state are subject to Jahn–Teller distortion in the low-spin d^7 ^2E state. This effect is best documented in structures of the Co(terpy)$_2^{2+}$ spin-equilibrium complex. The high-spin isomer is nearly octahedral, with a difference in Co–N bond lengths between the central and distal nitrogens of only 6 pm. In the Jahn–Teller distorted low-spin state this difference has increased to 21 pm (58).

A second class of complexes which display spin equilibria includes those with a tetragonal ligand field (152). Complexes with a strong in-plane ligand field tend to give low-spin configurations. Addition of fifth and sixth axial ligands can lead to spin-equilibrium complexes (91, 164, 165). Such complexes could participate in coordination-spin equilibria as well as the intramolecular spin-equilibria observed in some five- and six-coordinate examples. The dynamics of the spin equilibria in these tetragonal complexes has not yet been examined.

The rate of the spin state change for the octahedral cobalt(II) complexes is expected to be faster than that observed for the iron(II) and iron(III) complexes. In the cobalt(II) case the spin state change involves only one electron, that is $\Delta S = 1$. The ^2E and ^4T states are directly mixed by spin-orbit coupling (10, 163). The spin state transition should be adiabatic, with $\kappa = 1$, without any "spin-forbidden" barrier. Furthermore, the coordination sphere reorganization involves a change in bond length of 21 pm along only two bonds, instead of all six bonds as in iron complexes. Both of these factors lead to the prediction of rapid spin state interconversion.

This prediction is confirmed by observation of a very rapid relaxation of the spin equilibrium in Co(terpy)$_2^{2+}$ in solution. A relaxation time of less than 15 nsec was observed in a Raman laser temperature-jump experiment (14). This is consistent with the absence of any relaxation of the small excess sound absorption found in ultrasonic experiments. An upper limit of 0.2 nsec for the relaxation time in water at 298 K can be calculated from the magnitude of the excess absorption, which is

assumed to arise from a higher frequency relaxation process, and the values of ΔV^0 and ΔH^0 obtained from equilibrium measurements (18).

Such a short spin-equilibrium relaxation time raises the question of whether discrete spin state isomers exist. Their existence is affirmed by two observations. One is the persistence of electronic spectral bands typical of the low-spin ^2E state over a wide temperature range in solid samples (98). The other is the observation of EPR signals characteristic of the ^2E state in both solids and solutions between 4 and 293 K (98, 139). At very low temperatures EPR signals of both spin states can be observed simultaneously (98). At low temperatures hyperfine splitting into eight lines is observed from coupling with the $I = 7/2$ Co nucleus. As the temperature is raised the spectral features broaden and the hyperfine resolution is lost. This implies a relaxation process on the EPR time scale of 10^{10} sec^{-1}, or a relaxation time of the order 0.1 nsec, consistent with the upper limit set by the ultrasonic experiments.

These results make the observation of a "slower" relaxation time of 83 ± 23 nsec for the cobalt(II) complex [Co(N-NH(CH$_3$)-2,6-pyald)$_2$]$^{2+}$ rather unusual (141). This experiment was performed with the Raman laser temperature-jump technique in acetonitrile–methanol solutions. The slow relaxation was tentatively ascribed to coordination and solvation sphere reorganization barriers (141). Complex and solvent-dependent phenomena were found with this complex in the ultrasonic experiment. Ultrasonic absorption also occurs, however, with a related high-spin t-butyl-substituted complex (18). No relaxation was observed in aqueous solutions, which implies a relaxation time of less than 1 nsec. In methanol solutions multiple absorption curves are found. The interpretation of all of these observations remains uncertain. There may be partial ligand dissociation processes occurring, which could be correlated with the spin equilibrium. Alternatively, the spin-equilibrium relaxation could be hindered by steric and solvent effects. It is generally agreed that electronic factors arising from the spin state transition are unlikely to inhibit the spin equilibrium.

D. NICKEL(II)

Nickel(II) complexes display a variety of equilibria which involve spin state changes. Planar four-coordinate complexes are invariably diamagnetic. These can undergo an intramolecular isomerization to paramagnetic tetrahedral four-coordinate species. Alternatively, the planar complexes can coordinate additional ligands to form five- and six-coordinate paramagnetic complexes. The additional ligand molecules can be Lewis bases in solution, or solvent molecules, or, in par-

ticular cases, uncoordinated donor atoms of the ligand coordinated in the planar complex.

In this section the dynamics of spin equilibria of nickel(II) will be described, beginning with intramolecular planar–tetrahedral equilibria and continuing with coordination-spin equilibria, in which bond formation and dissociation become involved.

1. Planar–Tetrahedral Equilibria

Planar–tetrahedral equilibria of nickel(II) complexes were the first spin-equilibria for which dynamics were measured in solution. It had been known that such complexes were in relatively rapid equilibrium in solution at room temperature, for their proton NMR spectra were exchange averaged, rather than a superposition of the spectra of the diamagnetic and paramagnetic species. At low temperatures, however, for certain dihalodiphosphine complexes, it is possible to slow the exchange and observe separate resonances for the two species. On warming the lines broaden and coalesce and kinetics parameters can be obtained. Two research groups reported such results almost simultaneously in 1970 (99, 129). Their results and others reported subsequently are summarized in Table V.

A second method used to examine the same equilibria is the laser photoperturbation technique. Irradiation with a Q-switched laser pulse at 1060 nm depletes the tetrahedral isomer; irradiation at the doubled frequency of 530 nm depletes the planar isomer. In both cases the same relaxation time of 0.93(4) μsec is observed for reestablishment of the equilibrium.

A remarkable feature of these results is that they have been obtained only for the series of diphosphinedihalonickel(II) complexes. Of the many planar–tetrahedral spin equilibrium complexes of nickel(II), no others show dynamic effects in low-temperature NMR spectra. All of the complexes which remain in fast exchange at low temperature are bis(chelate) complexes, including aminotroponeimines, salicylaldimines, and β-ketoimines. This difference in ligand structure could affect the temperature dependence of the interconversion rates. Inspection of the reaction coordinate profile for one of the diphosphinedihalonickel(II) complexes (Fig. 6) reveals that the free energy of activation is dominated by a large enthalpy of activation. This accounts for the success in slowing the rate significantly by lowering the temperature. If the enthalpy of activation were somewhat smaller for the bis(chelate) complexes, resolution of the spectra in the low-temperature NMR experiments would not be possible.

There is no reason, however, why the dynamics of these systems should not be observable with more rapid techniques. Exploratory

TABLE V

DYNAMICS OF PLANAR–TETRAHEDRAL EQUILIBRIA OF NICKEL(II)

Complex	Solvent	T (K)	k_{31} (sec^{-1})	Reference
Ni(PPh$_2$Me)$_2$Br$_2$	CHCl$_3$	223	1.1×10^3	129
	CHCl$_3$	298	8.5×10^5	129
Ni(P(p-ClC$_6$H$_4$)$_2$Me)$_2$Br$_2$	CHCl$_3$	223	5.2×10^2	129
	CHCl$_3$	298	3.8×10^5	129
Ni(P(p-MeOC$_6$H$_4$)$_2$Me)$_2$Br$_2$	CHCl$_3$	223	6.8×10^1	129
	CHCl$_3$	298	1.4×10^5	129
Ni(P(p-MeOC$_6$H$_4$)$_2$Me)$_2$Cl$_2$	CHCl$_3$	223	3.3×10^3	129
	CHCl$_3$	298	1.6×10^6	129
Ni(PPh$_2$Me)$_2$Cl$_2$	CHCl$_3$	298	2.6×10^5	99
Ni(PPh$_2$Me)$_2$Br$_2$	CHCl$_3$	298	4.5×10^4	99
Ni(PPh$_2$Me)$_2$I$_2$	CHCl$_3$	298	2.9×10^6	99
Ni(PPh$_2$Et)$_2$Cl$_2$	CHCl$_3$	298	9.2×10^5	99
Ni(PPh$_2$Et)$_2$Br$_2$	CHCl$_3$	298	1.6×10^5	99
Ni(PPh$_2$Pr)$_2$Cl$_2$	CHCl$_3$	298	6.6×10^5	99
Ni(PPh$_2$Pr)$_2$Br$_2$	CHCl$_3$	298	1.3×10^5	99
Ni(PPh$_2$Bu)$_2$Cl$_2$	CHCl$_3$	298	7.5×10^5	99
Ni(PPh$_2$Bu)$_2$Br$_2$	CHCl$_3$	298	1.4×10^5	99
Ni(PCyp$_3$)$_2$Cl$_2$	CH$_2$Cl$_2$	223	4.9×10^3	134
	CH$_2$Cl$_2$	298	1.2×10^6	134
Ni(PCyp$_3$)$_2$Br$_2$	CH$_2$Cl$_2$	223	1.1×10^3	134
Ni(PPhCyp$_2$)$_2$Br$_2$	CH$_2$Cl$_2$	223	3.2×10^2	134
	CH$_2$Cl$_2$	298	1.5×10^5	134
Ni(PPh$_2$Cyp)$_2$Br$_2$	CH$_2$Cl$_2$	223	4.5×10^2	134
	CH$_2$Cl$_2$	298	1.5×10^5	134
Ni(PPh$_2$Cyh)$_2$Br$_2$	CH$_2$Cl$_2$	223	1.0×10^3	134
	CH$_2$Cl$_2$	298	9.3×10^5	134
Ni(dpp)Cl$_2$	CH$_3$CN	296	6×10^5	116
Ni(dpp)Br$_2$	CH$_3$CN	281	$\tau = 0.5\ \mu$sec	26
	CH$_3$CN	303	$\tau = 0.2\ \mu$sec	26

dpp

```
    Ph2
   ┌─P
  ⟨
   └─P
    Ph2
```

| Ni(4-MeSal)$_2$ | Cumene | 298 | $\tau \geq 0.2\ \mu$sec | 60 |

4-MeSal

```
        Me

         ⬡
   O          N-iPr
```

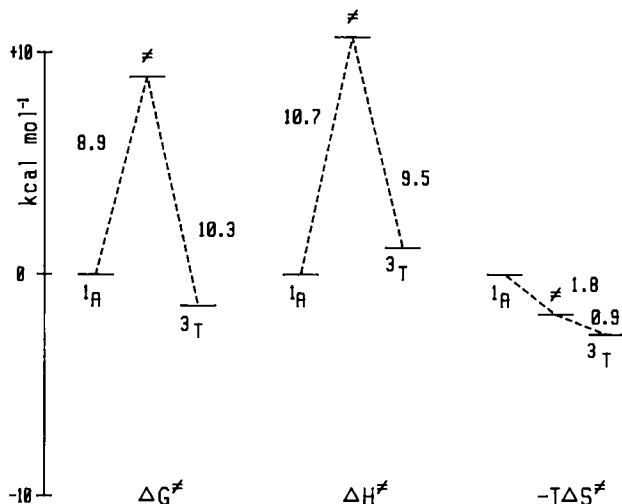| Ni(anisydyl-ati)$_2$ | Cumene | 298 | $\tau \geq 0.2\ \mu$sec | 60 |
| Ni(benzyl-ati)$_2$ | Cumene | 298 | $\tau \geq 0.2\ \mu$sec | 60 |

FIG. 6. Reaction coordinate profile for the planar–tetrahedral spin equilibrium of a diphosphinedihalonickel(II) complex.

experiments were undertaken with the ultrasonic resonance cell on cumene solutions of Ni(4-Mesal)$_2$, Ni(anisidyl-ati)$_2$, and Ni(benzyl-ati)$_2$. For the salicylaldimine complex a partial relaxation curve was observed, which indicates that relaxation occurs just to the low-frequency limit of this method, i.e., $\leqslant 1$ MHz or 160 nsec. For the aminetroponeimine complexes no excess sound absorption was found. From the properties of the solvent and the known thermodynamics of the equilibrium this again indicates that the relaxation time is longer than 200 nsec, corresponding to rate constants less than about 5×10^6 sec^{-1}. Application of photoexcitation techniques should be possible with these complexes, as has been demonstrated by photoexcitation experiments in closely related systems (5, 105).

The available evidence thus suggests that relaxation times for planar–tetrahedral equilibria in nickel(II) complexes in solution at room temperature fall in the range 0.1–10 μsec, corresponding to rate constants of the order $10^5 - 10^7$ sec^{-1}. These relaxation times are several orders of magnitude longer than those observed for octahedral spin equilibria. The reaction coordinate for the planar–tetrahedral equilibria is characterized by large enthalpies of activation for the reaction in both directions, in contrast with a relatively low enthalpy of activation for the high-spin to low-spin process in octahedral iron complexes.

There have been several theoretical analyses of the planar–tetrahedral interconversion process (49, 106, 107). The isomerization is not orbitally allowed without the inclusion of spin-orbit coupling, for the singlet ground state of the planar complex cannot correlate with the triplet ground state of the tetrahedral complex (70, 161). Inclusion of spin-orbit coupling mixes the ground states of both isomers sufficiently for the reaction coordinate to remain adiabatic; i.e., spin-orbit coupling for these $\Delta S = 1$ transitions mixes the two states so that there is an avoided crossing of the potential surfaces and the system remains on the lower energy surface from reactant to product.

An explanation for the slower rate and higher enthalpy of activation for the planar–tetrahedral isomerization compared with octahedral spin equilibria is apparent when the geometries of the processes are compared. For octahedral complexes the spin equilibrium produces a change in six metal–ligand bond lengths of not more than about 20 pm (0.2 Å). For the planar–tetrahedral isomerization the geometrical changes are much more extensive. Not only do the four bond lengths change by about 10 pm (0.1 Å), but there is a substantial change required as well along a bond bending or twisting coordinate. For a bis(bidentate) chelate complex the relative orientation of the two ligands must change by 90° between the planar and tetrahedral isomers. Motion of each donor atom with a metal–ligand bond length of 200 pm (2.00 Å) through an arc of 45° requires displacement by 157 pm (1.6 Å). This large geometry change undoubtedly contributes to the substantial activation enthalpy. There is no obvious explanation, however, for why the bis-bidentate chelate complexes undergo isomerization more rapidly than do the dihalophosphinenickel(II) complexes.

2. Planar–Octahedral Equilibria

Spin equilibria between diamagnetic planar four-coordinate complexes and paramagnetic five- or six-coordinate complexes clearly require bond formation and dissociation. The additional fifth and sixth ligands may be exogenous molecules or ions present in solution, solvent molecules themselves, or endogenous donors present in the planar complex as uncoordinated arms of a multidentate ligand. Although the thermodynamics of ligand addition to planar nickel(II) have been extensively studied, only recently have fast reaction techniques allowed examination of the dynamics (162).

Much of the focus of these studies has been on the relation between ligand substitution reaction mechanisms on octahedral nickel(II) and the dynamics of the planar–octahedral equilibria. For typical octa-
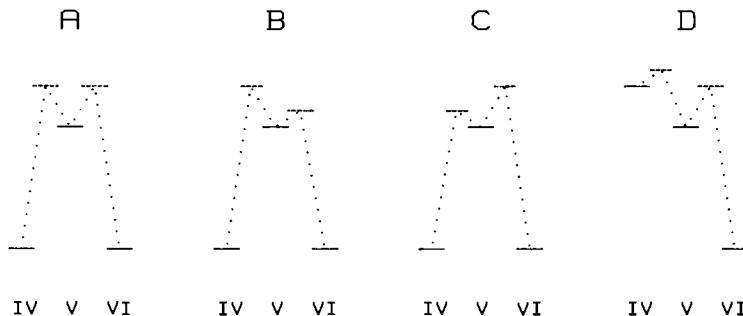
FIG. 7. Alternative reaction coordinate profiles for planar–octahedral equilibria of nickel(II).

hedral nickel(II) complexes, which undergo ligand substitution by a dissociative interchange mechanism, a five-coordinate species is a very unstable intermediate that closely resembles the transition state for substitution, and a four-coordinate species is of even higher energy (Fig. 7D). For complexes involved in a planar–octahedral equilibrium the four-coordinate species is stable, of energy comparable to the six-coordinate complex (Fig. 7A–C). Three possibilities exist for the reaction coordinate profile between the planar and octahedral complexes: in A (Fig. 7) the five-coordinate species closely resembles the transition state and is not an important intermediate; in B the interconversion between the planar and five-coordinate species is rate determining and the interconversion of five- and six-coordinate species is more rapid; in C the formation and dissociation of the six-coordinate, octahedral complex is rate determining and the interconversion of the planar and five-coordinate species is more rapid.

$$IV \underset{k_{54}}{\overset{k_{45}}{\rightleftharpoons}} V \qquad\qquad (10)$$

$$V \underset{k_{65}}{\overset{k_{56}}{\rightleftharpoons}} VI \qquad\qquad (11)$$

In some studies an assumption has been made about which of B or C (Fig. 7) is the rate-determining step, based more on prejudice about the role of the spin state change than on other evidence. At present it appears that only mechanism B can be distinguished from A and C. This is because mechanism B provides a pathway for ligand (or solvent) exchange from the six-coordinate complex, which is more rapid than the planar–octahedral interconversion and which can be observed by NMR

independently. Thus if ligand (or solvent) exchange is more rapid than the planar–octahedral equilibrium, mechanism B obtains. In contrast, mechanisms A and C cannot be distinguished, unless the five-coordinate intermediate is particularly stable and accumulates. Otherwise, the ligand or solvent molecule does not have a sufficiently long residence time in the five-coordinate species to be relaxed, even if the five-coordinate species is paramagnetic.
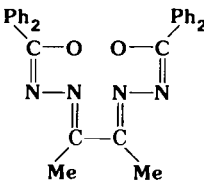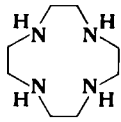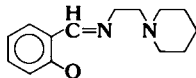
The addition and dissociation of pyridine and substituted pyridine molecules to a planar nickel(II) complex with a quadridentate N_2O_2 ligand have been studied by the microwave temperature-jump technique in chlorobenzene solvent (38). The data were interpreted with the assumption of mechanism C (Fig. 7), i.e., that k_{65} is the smallest rate constant. Subsequently, however, ^{14}N NMR was used to measure the rate of pyridine exchange from the octahedral complex (138). The rates are the same for the two different experiments within a factor of two. This observation excludes mechanism B and is consistent with either mechanism A or C. The rate constants have consequently been presented in Table VI as k_{64}.

In contrast, solvent exchange on $Ni([12]aneN_4)(H_2O)_2^{2+}$ is greater than 100 times more rapid than the planar–octahedral equilibrium (33). Mechanism B obtains. This apparently arises because the ligand undergoes stereochemical reorganization between the planar complex and a cis configuration in the six-coordinate complex. In both $Ni(2,3,2-tet)(H_2O)_2^{2+}$ and $Ni(cyclam)(H_2O)_2^{2+}$ water exchange is about a factor of 10 faster than the planar–octahedral equilibrium. In $Ni(trien)(H_2O)_2^{2+}$, however, water exchange proceeds at the same rate as the planar–octahedral interconversion.

These latter three tetraaminenickel(II) complexes are thought to possess a trans-octahedral geometry in the six-coordinate state. For these complexes little distinction can be inferred between mechanisms A, B, and C (Fig. 7). Both the four–five and five–six coordination number changes proceed at about comparable rates. A spin state change occurs in one of these steps. It is likely that the five-coordinate intermediate is paramagnetic, by analogy with the stable five-coordinate complexes described below. Hence the spin state change occurs in the four–five coordination step. This step is not substantially slower than the five–six coordination change, however, which does not involve a spin state change. This inference can be rationalized from the energetics of the reaction as follows. Dissociation of a ligand from the six-coordinate complex is endothermic, producing an unstable five-coordinate, but still high-spin, complex. The endothermic dissociation of the second ligand is compensated by the shortening of the in-plane

TABLE VI
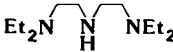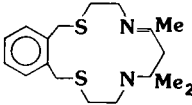
DYNAMICS OF PLANAR–OCTAHEDRAL EQUILIBRIA AT 298 K

Planar complex	Octahedral complex	Solvent	k_{64} (sec^{-1})	Reference
Ni(2,3,2-tet)$^{2+}$	Ni(2,3,2-tet)(H$_2$O)$_2$$^{2+}$	H$_2$O	4.9×10^5	85
		H$_2$O	$k_{65} = 8 \times 10^6$	127
	2,3,2-tet	H$_2$N N N NH$_2$ / H H		
Ni(trien)$^{2+}$	Ni(trien)(H$_2$O)$_2$$^{2+}$	H$_2$O	1×10^6	85
		H$_2$O	$k_{65} = 1.1 \times 10^6$	135
Ni(bbh)	Ni(bbh)(py)$_2$	C$_6$H$_5$Cl	3.5×10^4	38
		py	5.6×10^4	138
	Ni(bbh)(2-Mepy)$_2$	C$_6$H$_5$Cl	3.8×10^5	38
		2-Mepy	8.5×10^5	138
	bbh	Ph$_2$ C—O O—C Ph$_2$ / N—N N—N / C—C / Me Me		
Ni([12]aneN$_4$)	Ni([12]aneN$_4$)(H$_2$O)$_2$$^{2+}$	H$_2$O	1.5×10^4	33
		H$_2$O	$k_{65} = 4.2 \times 10^7$	33
	[12]aneN$_4$			
Ni(cyclam)$^{2+}$	Ni(cyclam)(H$_2$O)$_2$$^{2+}$	H$_2$O	3.6×10^6	60
		H$_2$O	$k_{65} = 4 \times 10^7$	127
Ni(Me$_4$cyclam)$^{2+}$	Ni(Me$_4$cyclam)(H$_2$O)$_2$$^{2+}$	H$_2$O	2.8×10^7	13
Ni(Salpip∼)$_2$	Ni(Salpip)$_2$	Cumene	8.0×10^6	61
	Salpip			

metal–ligand bonds accompanying the spin state change. This confers the additional stability on the four-coordinate complex, which lowers its energy from that which obtains in the octahedral substitution mechanism (Fig. 7D). The spin state change affects the energetics and dynamics of the equilibria, but only as it affects the thermodynamics.

TABLE VII

DYNAMICS OF PLANAR—FIVE-COORDINATE EQUILIBRIA OF NICKEL(II)

Planar complex	Five-coordinate complex	Solvent	k_{54} (sec^{-1})	Reference
$Ni(Et_4dien)Cl^+$	$Ni(Et_4dien)Cl_2$	CH_3CN	7×10^5	*78, 27*
	Et_4dien	Et_2N $\overset{N}{H}$ NEt_2		
$Ni(AEX)^{2+}$	$Ni(AEX)(H_2O)^{2+}$	H_2O	1.5×10^7	*28*
	AEX			
$Ni(Me_4cyclam)^{2+}$	$Ni(Me_4cyclam)(CH_3CN)^{2+}$	CH_3CN	4.0×10^6	*75a*
$Ni(Me_4cyclam)^{2+}$	$Ni(Me_4cyclam)(DMF)^{2+}$	DMF	1.6×10^7	*104*

There is no evidence that the reactions are in any way nonadiabatic, i.e., that the electronic aspects of the spin state change inhibit the dynamics.

Some diamagnetic planar nickel(II) complexes add only one ligand to form paramagnetic five-coordinate species. The dynamics of several of these equilibria have been examined by photoperturbation or NMR methods. The rate constants present in Table VII are of the order 10^6 sec^{-1} for the dissociation of the ligand from the five-coordinate species. These rates are comparable with those of the planar–octahedral equilibria and are consistent with the mechanistic interpretation presented above.

V. Solid-State Dynamics

Only three aspects of the dynamics of spin equilibria in the solid state will be reviewed. One is the classification of the rates of spin interconversion based on spectroscopic properties observed in the solid. The second is the direct measurement of spin state lifetimes in crystals and powders. The third, the comparison of these with the dynamics observed in solutions, will be described in the course of the discussion.

The temperature dependence of the spin state populations in solids, as measured by magnetic susceptibility or any of the other properties which differ with the spin state, falls into two classes. In one class there

is a gradual transition from one spin state to the other, more or less following a Boltzmann distribution, just as is observed in solutions. In the other class there is an abrupt change between the spin states at a particular transition temperature, often with hysteresis as the temperature is raised and lowered. In this second class the spin state transition is clearly a cooperative property of the lattice as well as of the discrete spin-equilibrium complex. The mechanisms of these cooperative spin state transitions have been extensively investigated and reviewed (65, 95) and will not be discussed further here. Attention will be focused on the gradual transitions which potentially reflect properties of the individual complexes. Even in these cases some degree of cooperativity can remain (57, 74).

A. LIFETIME LIMITS

The physical and spectroscopic properties of a spin-equilibrium complex can appear to be either the average or the superposition of the properties of the separate spin states. Which occurs is dependent on the time scale of the observation relative to the relaxation time of the equilibrium. Thus the electronic and vibrational spectra always appear as a superposition of the two isomers because each spin state possesses a distinctive potential energy surface with its characteristic electronic and vibrational properties. On the other hand, the NMR spectra appear as the average of the spectra of the two spin states, for all but the slowest interconversions, because the frequency of the interconversion is high compared with the frequency differences of the chemical shifts or the inverse of the spin relaxation times of the two isomers.

The two techniques which have been used effectively to set limits on the rates of spin state interconversions are Mössbauer and EPR spectroscopies. As described in Section III,E, the lifetime of the excited nuclear state involved in the Mössbauer effect is 10^{-7} second. Thus the observation of the Mössbauer spectrum can immediately classify the spin state lifetime as greater than or less than 10^{-7} second. Both conditions have been observed, as was described in Section III,E.

There is some evidence that the strength of intermolecular forces determines the degree of cooperativity and the rate of spin state interconversion in the lattice (154, 155). This is a reasonable hypothesis, for it assumes a continuum of behavior, from very weak interactions, which reflect intramolecular properties, to strong intermolecular forces, which cause cooperative phase transitions and abrupt spin state changes. Neutral complexes with a molecular lattice and little or no hydrogen bonding between the molecules, such as some iron(III)

dithiocarbamate complexes, undergo rapid spin interconversion even in the solid state. Neutral complexes with larger volume changes between the isomers, such as the iron(II) pyrazolylborate complexes, which cause a greater reorganization of the crystal lattice, undergo slow interconversion on the Mössbauer time scale (67, 68). As hydrogen bonding causes the lattice to become more of a network, cooperativity increases and the rates of spin state interconversion decrease. Because the lattice properties and the intramolecular requirements of the spin state transition depend on a number of different factors, there will be no simple relationship between the intrinsic rate and the solid-state rate. Indeed, there is increasing evidence that solvation effects influence the properties of the spin equilibrium even in solution (115), as would be expected.

The EPR spectrum of a spin-equilibrium complex can be used to establish a lower limit to the spin state lifetimes of the order of 10^{-10} second. In an important paper in 1976, Hall and Hendrickson reported observation of EPR signals for both the high-spin and the low-spin isomers of iron(III) dithiocarbamate complexes at 4–12 K as powders, glasses, and doped solids (71). This resolved the question whether these complexes possess distinct high-spin and low-spin states. It also sets a lower limit on their interconversion lifetimes. Similarly, the observation of signals for both the high-spin and low-spin states of $[Co(terpy)_2^{2+}]$ (97) leads to the same conclusions about this complex. In both cases the interconversion rates in solution have proved too fast to measure, with lifetimes of less than 10^{-9} second indicated. The solution measurements were undertaken, of course, at room temperature and the EPR measurements at close to 4 K. Significant differences in the rates of solid and solutions at room temperature are still possible.

B. MEASURED RATES

Mössbauer spectroscopy can only be used to obtain rates of interconversion if the lifetimes are close to 10^{-7} second. As described in Section III,E a few examples satisfying this condition have been found. Some questions remain over the quantitative interpretation of the data. Nevertheless, spin-equilibrium relaxation lifetimes have been estimated from Mössbauer temperature-dependent linewidths for two salts of an iron(III) complex, $[Fe(acpa)_2]^+$. The lifetimes are of the order 10^{-5}–10^{-7} second over temperature ranges from 100 to 300 K (109, 111).

Interconversion rates have also been measured recently using a photoperturbation technique on solid samples. Irradiation of a sample

at very low temperatures causes population of the higher energy spin state with an efficiency of 0.1–1% (*40, 41, 73, 77*). This "light-induced excited spin state trapping" occurs at temperatures too low for the thermally activated back intersystem crossing reaction to occur. On raising the temperature to ~60 K this process occurs within minutes (*39*). The relaxation is not first order, but the sample of the iron(II) complex undergoes a cooperative spin state transition. The effect has also been observed with the complex $[Fe(2-pic)_3]Cl_2 \cdot EtOH$, which undergoes a gradual spin state change as a crystal. In this case the relaxation of the photoperturbed equilibrium occurs at 25–30 K within an hour (*39*). No rates have yet been reported, but this appears to be a promising general method with convenient relaxation times for studying the interconversion kinetics in solid samples. The extrapolation to room temperature conditions is too long, however, for reliable, detailed comparisons to be made between solids and solutions. There is no reason, however, why increasingly sensitive nanosecond photometric detection will not enable the photoperturbation technique to be used on solids at room temperature as it has been used on solutions.

VI. Summary and Interpretation

The dynamics of spin equilibria in solution are rapid. The slowest rates are those for coordination-spin equilibria, in which bonds are made and broken; even these occur in a few microseconds. The fastest are the $\Delta S = 1$ transitions of octahedral cobalt(II) complexes, in which the population of the $e_g^* \ \sigma$ antibonding orbital changes by only one electron; these appear to occur in less than a nanosecond. For intramolecular interconversions without a coordination number change, the rates decrease as the coordination sphere reorganization increases. Thus the $\Delta S = 2$ transitions of octahedral iron(II) and iron(III) are slower than the $\Delta S = 1$ transitions of cobalt(II), and the planar-tetrahedral equilibria of nickel(II) are slower again, with lifetimes of about a microsecond.

A. OCTAHEDRAL $\Delta S = 2$ EQUILIBRIA

The spin equilibria of octahedral iron(II) complexes are the best studied examples in both the solid state and in solution. Both the low-spin ^1A and the high-spin ^5T states are regular octahedra, so the

transition can be considered a one-dimensional problem in the totally symmetric metal–ligand stretching coordinate. The bond length change is large (Table I), with an average difference of 20 pm per bond between the high-spin and low-spin states. Nevertheless, the rates of interconversion are rapid. The relaxation times observed for eight different complexes with the use of three different techniques span the narrow range from 27 to 120 nsec.

These relaxation times correspond to rates which are about 10^6 slower than the thermal vibrational frequency of $6 \times 10^{12} \sec^{-1}$ ($k_B T/h$) obtained from transition state theory. The question arises how much, if any, of this free energy of activation barrier is due to the spin-forbidden nature of the $\Delta S = 2$ transition. This question is equivalent to evaluating the transmission coefficient, κ, that is, to assess quantitatively whether the process is adiabatic or nonadiabatic.

It is not possible to evaluate κ directly, for it appears with the entropy of activation in the temperature-independent part of the rate constant. An estimate of κ requires an extrathermodynamic assumption. In two cases of iron(II) spin equilibria examined by ultrasonic relaxation the temperature dependence of the rates was precisely determined. If the assumption is made that all of the entropy of activation is due to a small value of κ, minimum values of 10^{-3} and 10^{-4} are obtained. Because there is an increase in entropy in the transition from the low-spin to the high-spin states, this assumption is equivalent to assuming that the transition state resembles the high-spin state. There is now evidence that this is not the case. Volumes of activation indicate that the transition state lies about midway between the two spin states. This is a more chemically reasonable and likely situation than the limiting assumption used to evaluate κ. In this case the observed entropy of activation includes some "chemical" contributions which arise from increased solvation and decreased vibrational partition functions as the high-spin state is compressed to the transition state. Consequently, the minimum value of κ is increased and is unlikely to be less than about 10^{-2}.

The singlet and quintet states are not mixed directly by spin-orbit coupling. According to this description the intersystem crossing should be completely forbidden. The two spin states are mixed, however, through second-order coupling with the excited triplet state. Thus the energy of that state is important in evaluating the extent of mixing of the singlet and quintet states and the magnitude of κ. Estimates of mixing of the order of $10–100 \text{ cm}^{-1}$ have been made (23, 45). According to the Landau–Zener description of surface crossings, this corresponds to values of κ of the order 10^{-3} to 10^{-1}, in good agreement with the

observations. Alternatively, a description of the reaction as a multiphonon radiationless transition has been given (23). Rate constants of 10^9 sec^{-1} are calculated, in reasonable agreement with the observed 10^7 sec^{-1}.

The description of the ^2T–^6A spin equilibrium of octahedral iron(III) complexes is similar to that for iron(II). Again the $\Delta S = 2$ transition occurs between octahedral states along a single metal–ligand coordinate. Again there is no direct mixing between the states, but coupling through the intermediate quartet state. There are fewer structural data for iron(III) complexes, but the difference in bonds lengths between the spin states appears to be somewhat smaller, with an average among three structures of 14 pm (Table I). If this is correct it would account for the somewhat faster rates observed for the relaxation of the spin equilibrium. For three complexes the relaxation times are 2–5 nsec, an order of magnitude shorter than those observed for iron(II). It should be noted that all three of these complexes are derived from a common N_4O_2 ligand structure and that, therefore, these results may not be representative. Minimum values of κ of 10^{-2} to 10^{-3} have again been made with the assumption that the transition state resembles the high-spin state. A more reasonable transition state intermediate between the doublet and sextet geometries will increase κ to 10^{-2} to 10^{-1}, again in agreement with estimates of the mixing between the spin states (94).

The conclusion is that these spin equilibria are only weakly "spin forbidden," with nonadiabatic transmission coefficients not smaller than 10^{-2}. The activation free energy is dominated by the inner-sphere reorganization energy which arises from the substantial bond length changes which accompany the transfer of two e_g* electrons. The dynamics can be properly described as an "intramolecular electron transfer reaction dominated by inner-sphere effects" (45). Solvent effects are small. In outer-sphere electron transfer reactions solvent reorganization is an important contributor to the activation free energy because of the transfer of charge. In spin equilibria the electrons are only redistributed on a single center. Solvent effects will be smaller and dependent on differences in solvation between the two spin states. These will include not only the change in volume between the two spin states, but also specific differences in hydrogen bonding in some cases.

B. OCTAHEDRAL $\Delta S = 1$ EQUILIBRIA

If the above analysis is correct, spin equilibria with $\Delta S = 1$ will relax significantly more rapidly than those with $\Delta S = 2$, for two reasons. One is that the transmission coefficient κ will be close to unity, because

spin-orbit coupling directly mixes the two spin states. The second is that the coordination sphere reorganization barrier is lower, because the two spin states differ by only a single e_g^* electron.

The available evidence, which is limited to cobalt(II) complexes, is ambiguous. Crystallographic evidence on the $[Co(terpy)_2]^{2+}$ complexes indicates an average bond length difference of 12 pm between the high-spin and low-spin states. This is substantially less than the 20 pm found in iron(II) complexes, but not significantly different from the 14 pm seen in some iron(III) examples. Moreover, because the low-spin cobalt(II) ^2E state is subject to Jahn–Teller distortion, two of the six bond lengths differ by 21 pm, while the other four differ by only 7 pm (Table I). On a harmonic potential surface the energy required to distort the bonds to the transition state depends on the square of the distance, so the large difference for two of the bonds will contribute more than the average difference would imply. This suggests that the difference in spin-equilibria relaxation times between iron(III) and cobalt(II) might depend largely on the difference in κ.

The dynamics results are insufficient to resolve this question. For $[Co(terpy)_2]^{2+}$ the spin state relaxation appears to occur in only a few tenths of a nanosecond, consistent with the prediction that it could be an order of magnitude faster than that of iron(III). On the other hand, some relaxation process in another [Schiff base cobalt(II)] complex occurs with a slower relaxation time of 83 nsec. Until more data are acquired, this question must remain unresolved. It is a reasonable surmise, however, that these reactions are adiabatic.

C. PLANAR–TETRAHEDRAL $\Delta S = 1$ EQUILIBRIA

If the electronic spin state change were the critical determinant of the dynamics of spin equilibria, then the $\Delta S = 1$ equilibration between planar and tetrahedral nickel(II) isomers would occur more rapidly than equilibration of the octahedral $\Delta S = 2$ spin states. This is not observed. Even though the $\Delta S = 1$ transition is most likely adiabatic, the large coordination sphere reorganization energy requirement causes these nickel(II) isomerizations to occur relatively slowly, with relaxation times of the order of a microsecond.

For those which have been studied by low-temperature NMR, in the dihalodiphosphinenickel(II) family, the activation parameters are characterized by a high enthalpy of activation. This is consistent with a large reorganization energy requirement. Although the bond length difference between the spin states is only 5 pm, there is a large change

in the interligand bond angles between the planar and tetrahedral isomers. Because the energy required for distortion along a harmonic surface increases as the square of the displacement, a large bond angle change can produce a large activation energy barrier.

Only a few examples of these planar–tetrahedral equilibria have been successfully investigated and there remain unanswered questions about the dynamics. Nevertheless, it seems reasonable to regard these equilibria as intramolecular isomerizations in which the spin state change is not an important factor in the dynamics. Electron spin affects the bonding, geometry, and thermodynamics of the two isomers, but there is apparently sufficient mixing of the singlet and triplet states to allow their interconversion to be adiabatic.

D. PLANAR–OCTAHEDRAL $\Delta S = 1$ EQUILIBRIA

Analysis of these equilibria is more complex than those described above because the planar–octahedral reactions are not intramolecular, but involve formation and dissociation of metal–ligand bonds. The processes are most likely to be adiabatic, a consequence of spin-orbit coupling between the singlet and triplet states. All of the dynamics have been observed with nickel(II). Consequently, the reactions observed for nickel(II) are usefully regarded in the context of the model for dissociative ligand substitution on that metal ion. The presence of the nearly equienergetic planar singlet state reduces the energy of the activated complex and increases the rate of the ligand dissociation reaction. The role of the five-coordinate intermediate is not clear, but for most of the reactions which have been examined it appears to be of high energy and not to accumulate. There is no evidence to indicate that electronic aspects of the spin state transition produce a rate-limiting process, except insofar as they contribute to the coordination sphere reorganization energy.

VII. Implications

The conclusions described in the previous section are inferred from a relatively small number of observations of spin-equilibrium dynamics. Nevertheless, they are internally self-consistent and also compatible with a much wider set of observations derived from studies of electron transfer reactions of metal complexes. For these reasons there is hope that they possess some generality and can be applied to other systems.

There are a few examples of spin equilibria with other metal ions which have not been mentioned above. In cobalt(III) chemistry there exist some paramagnetic planar complexes in equilibrium with the usual diamagnetic octahedral species (22). The equilibria are the converse of the diamagnetic-planar to paramagnetic-octahedral equilibria which occur with nickel(II). Their interconversions are also presumably adiabatic. Preliminary observations indicate relaxation times of tens of microseconds, consistent with slower ligand substitution on a metal ion in the higher (III) oxidation state (120).

Examples of spin equilibria among d^4 ions are rare. At least one Mn(III) example is known, which shows a cooperative spin state transition at low temperature (142a). No dynamics have been reported. The spin state transition has $\Delta S = 1$ and is therefore probably adiabatic. There is likely to be a substantial coordination sphere reorganization energy, however, for in this case the high-spin state is Jahn–Teller distorted, so there will be a large difference in some metal–ligand bond lengths between the two spin states.

A second example is the recently reported singlet–triplet equilibrium in a Mo(II) complex, cis-[Mo(bipy)$_2$(OPr$_i$)$_2$] (31). The interpretation of the magnetism is complicated by the possibility that the equilibrium is not entirely metal centered, but involves charge transfer to the bipyridyl ligands. Because a strong field is required to spin pair the d^4 configuration, however, it is not impossible that examples exist among Mo(II) chemistry. The possible dynamics are subject to considerations similar to those which apply to Mn(III).

Spin equilibria among organometallic complexes are also rare. Generally the ligand fields are too strong to allow population of the high-spin state. A well-documented exception occurs with bis(methylcyclopentadienyl)manganese(II), dimethylmanganocene. EPR and solution magnetic moments have established a ^2E–^6A equilibrium for this d^5 ion, analogous to that observed for iron(III) complexes (4, 150). An electron diffraction study gave a difference of 28 pm in the Mn–C distances in the two states (1). No dynamics have been reported; studies both in the solution and in the gas phase would be most interesting.

A. Reaction Mechanisms

1. Racemization and Isomerization

Spin state transitions have been invoked in explaining a number of reaction mechanisms. One is the intramolecular racemization of [Fe(phen)$_3$]$^{2+}$. The complex exists in the low-spin state, but expansion

of the coordination sphere along a reaction coordinate for an intramolecular twisting racemization could reduce the ligand field enough to populate the high-spin state. Evidence for this hypothesis has been advanced from measurements of volumes of activation. These are large and positive $(+15 \text{ cm}^3 \text{ mol}^{-1})$ for both racemization and aquation, in contrast with values close to zero for the analogous reactions of $[\text{Ni(phen)}_3]^{2+}$ (100). The volume of activation for the iron(II) complex is comparable to those found for the spin equilibria of octahedral iron complexes (Table II). This lends credence to the hypothesis. A theoretical analysis of the mechanism has been presented, which includes an estimate of the transmission coefficient, κ, of the order of 10^{-1} (132).

Similar invocations of spin equilibria have been made for the racemization of a tris(dithiocarbamate)cobalt(III) complex (101) and a sexadentate iron(II) complex (32), and the isomerization of a cis-bis(phenanthroline)iron(II) complex (133). In the last case a semantic difficulty over the definition of rate constants obscures the argument. When the two spin states are not in thermal equilibrium, the forward and reverse rate constants are of course no longer nearly equal. The rate constant in the forward direction, k_{15}, from the ground state to the excited state, will be much less than in the reverse direction, from the excited state to the ground state, k_{51}. For a $\Delta S = 2$ transition in iron(II), k_{51} is likely to be of the order of 10^7 sec^{-1}. The value of k_{15} will be less than that of k_{51} by the energy difference between the ground and excited states. The reported rate for the isomerization reaction indicates that this energy difference between the ^1A and ^5T states must be less than $2000-2500 \text{ cm}^{-1}$. Only if the rate of the isomerization reaction in the excited state is greater than or competitive with k_{51} can the measured rate be identified with k_{15}. Since k_{51} is of the order of 10^7 s^{-1}, this condition is unlikely to be met. It is confusing, therefore, to identify the forward rate constant as that appropriate for a spin state change, because of the large thermal barrier to be surmounted.

2. Electron Transfer

Similar considerations apply to the role of spin equilibria in electron transfer reactions. For many years spin state restrictions were invoked to account for the slow electron exchange between diamagnetic, low-spin cobalt(III) and paramagnetic, high-spin cobalt(II) complexes. This explanation is now clearly incorrect. The rates of spin state interconversions are too rapid to be competitive with bimolecular encounters, except at the limit of diffusion-controlled reactions with molar concentrations of reagents. In other words, a spin equilibrium with a

relaxation time of a few nanoseconds will always remain in equilibrium, even if one of the spin states participates in some bimolecular reaction. *Spin state changes are not rate determining in bimolecular reactions.* This conclusion could always have been inferred from the rate law for the cobalt(III)–cobalt(II) electron transfer reaction, for if the spin state change had been rate determining, the rate law would have been first order, not second order.

Spin restrictions may still affect the rate of electron transfer. If electron exchange between the ^1A and ^4T states is spin forbidden, then a spin-equilibrium transition prior to electron transfer is required. The rate of bimolecular electron exchange from this excited spin state will always be much lower than the thermal depopulation of this state to the other spin isomer, just as the rate of isomerization described above is less than the depopulation of the excited iron(II) spin state. For the cobalt(III)–cobalt(II) electron exchange, the spin state change is most likely to be in the cobalt(II) state from ^4T to ^2E. Note that this severely complicates the prediction of the rate because the ^2E state is subject to Jahn–Teller distortion. The usual one-dimensional analysis of the inner-sphere reorganization energy is not applicable. Both cobalt(II) and cobalt(III) will distort, requiring a two-dimensional analysis. In this sense spin restrictions affect the electron transfer by selecting a particular reaction coordinate. Alternatively, if the ^2E and ^1A surfaces were to cross above the ^4T and ^1A surfaces (Fig. 7B), spin restrictions would affect the rate by imposing a higher enthalpy of activation on the reaction. In neither case, however, would spin state changes be rate determining.

3. Substitution

Just as expansion of the coordination sphere by transition from the low-spin to the high-spin state enhances isomerization and racemization, so too should it enhance the rate of ligand substitution. Unpublished observations on the ligand substitution of $[Fe(pyim)_3]^{2+}$, which is coupled with its spin equilibrium, indicate that it is the high-spin state which preferentially undergoes the substitution reaction, as expected (*117*).

Less expected, perhaps, are results on substitution reactions of four-coordinate nickel(II) chelate complexes which occur in equilibrium between planar and tetrahedral isomers. Despite the longer bond lengths of the tetrahedral isomers, it is the planar isomers which undergo the substitution reactions (*140*).

B. Excited States

Spin equilibria are thermal intersystem crossing processes. The "ground state" and the "excited state" lie within a few hundred wavenumbers of each other and both are thermally populated. There are two photophysical processes in excited states related to the dynamics of thermal spin equilibria. One is the radiationless deactivation of an excited state to a ground state of different spin multiplicity. The other is intersystem crossing between excited states.

The results obtained from thermal spin equilibria indicate that $\Delta S = 1$ transitions are adiabatic. The rates, therefore, depend on the coordination sphere reorganization energy, or the Franck–Condon factors. Radiationless deactivation processes are exothermic. Consequently, they can proceed more rapidly than thermally activated spin-equilibria reactions, that is, in less than nanoseconds in solution at room temperature. Evidence for this includes the observation that few transition metal complexes luminesce under these conditions. Other evidence is the very success of the photoperturbation method for studying thermal spin equilibria; intersystem crossing to the ground state of the other spin isomer must be more rapid than the spin equilibrium relaxation in order for the spin equilibrium to be perturbed.

There are of course many examples of metal complexes with excited state lifetimes of longer than a few nanoseconds. These often involve vertical transitions, however, as in the well-studied case of the ^2E excited state of chromium(III) (51). The inferences to be drawn from spin-equilibrium dynamics apply only to nonvertical transitions along a metal–ligand reaction coordinate. These considerations imply that intersystem crossing between excited states is a closer analogy with thermal spin equilibria. The rates of such $\Delta S = 1$ processes should be determined by their thermodynamics and reorganization energy requirements, but not be limited by changes in spin multiplicity. This difference from singlet–triplet transitions in organic molecules arises from the larger spin-orbit coupling in transition metal complexes.

Even $\Delta S = 2$ transitions in excited states can be rapid. In ground state spin equilibria these transitions can be nonadiabatic due to the requirement of mixing through spin-orbit coupling with excited intermediate spin states. In photophysical processes these excited states can actually be populated. Again this conclusion follows from the success of photoperturbation methods applied to $\Delta S = 2$ spin equilibria. For example, excitation of the singlet state of iron(II) results in detectable population of the quintet spin-equilibrium state more rapidly than

the nanosecond relaxation between the singlet and quintet spin-equilibrium states. The most likely cause of this is very rapid crossings from the excited singlet state to an intermediate triplet state to a quintet state. The efficiency of this process is high, with quantum yields at low temperatures in crystals of 0.1–1% (*73, 131*). This implies nearly adiabatic intersystem crossing.

C. PORPHYRINS AND HEME PROTEINS

Spin equilibria are an important feature of the chemistry of porphyrins and heme proteins. The extensive literature on this subject cannot be reviewed here. Only some relevant implications from the studies of spin equilibria in metal complexes will be described.

The spin equilibria of iron(II) and iron(III) in a porphyrin coordination environment combine the features of $\Delta S = 2$ equilibria with the coordination-spin equilibria of nickel(II). There is often a coordination number change from five-coordinate high-spin to six-coordinate low-spin geometries. Consequently, there is substantial reorganization energy required for bond formation and dissociation. In addition, the $\Delta S = 2$ transitions are potentially nonadiabatic.

There is an important feature of porphyrin chemistry which increases the adiabaticity of these transitions. As the ligand field is distorted from octahedral to tetragonal, the energy of the intermediate spin states, triplet for iron(II) and quartet for iron(III), is lowered. In some cases these intermediate spin states become the ground states. These possess an intermediate magnetic moment which does not display the same temperature dependence as the Boltzmann equilibrium between high-spin and low-spin states. In other cases equilibria may exist between these intermediate spin states and either the high-spin or low-spin isomers. These possibilities obviously complicate the analysis and description of the magnetic and related properties of such complexes.

The presence of these low-lying intermediate spin states, however, also increases the mixing through spin-orbit coupling between the high-spin and low-spin states. By perturbation theory this mixing depends on the square of the energy difference between the ground states and the intermediate excited state. Since in octahedral iron complexes the $\Delta S = 2$ spin equilibria are estimated to be nonadiabatic only by a factor not less than 10^{-2}, the low-lying intermediate spin states should make spin equilibria in porphyrins and heme proteins adiabatic or nearly so.

If this interpretation is correct, then the rate of spin state transitions in these systems will depend on the reorganization energy requirements. Two examples will be described. Ferric myoglobin undergoes a

spin equilibrium between a low-spin state in which a small molecule such as hydroxide or azide is coordinated in the sixth position and a high-spin state in which this ion is dissociated from the iron(III) but still located within the heme pocket. This equilibrium is estimated to have a relaxation time of about 20 ns (46). In contrast, ferricytochrome c undergoes a spin equilibrium in acidic solution in which the sixth endogenous ligand methioine dissociates. This equilibrium has a relaxation time of 100 μsec (48). The difference in rates arises from the difference in the reorganization energies required.

REFERENCES

1. Almenningen, A., Samdal, S., and Haaland, A., *J. Chem. Soc. Chem. Commun.* 14 (1977).
2. Ameen, S., *Rev. Sci. Instrum.* **46,** 1209 (1975).
3. Ammeter, J. H., *Nouv. J. Chim.* **4,** 631 (1980).
4. Ammeter, J. H., Bucher, R., and Oswald, N., *J. Am. Chem. Soc.* **96,** 7833 (1974).
5. Amir-Ebrahimi, V., and McGarvey, J. J., *Inorg. Chim. Acta* **89,** L39 (1984).
6. Bacci, M., *Inorg. Chem.* **25,** 2322 (1986).
7. Barefield, E. K., Bianchi, A., Billo, E. J., Connolly, P. J., Paoletti, P., Summers, J. S., and van Derveer, D. G., *Inorg. Chem.* **25,** 4197 (1986).
8. Barefield, E. K., Busch, D. H., and Nelson, S. M., *Q. Rev. Chem. Soc.* **22,** 457 (1968).
9. Barefield, E. K., Freeman, G. M., and Van Derveer, D. G., *Inorg. Chem.* **25,** 552 (1986).
10. Barraclough, C. G., *Trans. Faraday Soc.* **62,** 1033 (1966).
11. Batschelet, W. H., and Rose, N. J., *Inorg. Chem.* **22,** 2083 (1983).
12. Beattie, J. K., Binstead, R. A., and West, R. J., *J. Am. Chem. Soc.* **100,** 3044 (1978).
13. Beattie, J. K., Kelso, M. T., Moody, W. E., and Tregloan, P. A., *Inorg. Chem.* **24,** 415 (1985).
14. Beattie, J. K., Sutin, N., Turner, D. H., and Flynn, G. W., *J. Am. Chem. Soc.* **95,** 2052 (1973).
15. Becker, E. D., "High Resolution NMR," 2nd Ed., pp. 44–46. Academic Press, New York, 1980.
16. Beitz, J. V., Flynn, G. W., Turner, D. H., and Sutin, N., *J. Am. Chem. Soc.* **92,** 4130 (1970).
17. Bernasconi, C. F., "Relaxation Kinetics." Academic Press, New York, 1976.
18. Binstead, R. A., Ph.D. thesis, University of Sydney, 1979, and unpublished observations, 1986.

19. Binstead, R. A., and Beattie, J. K., *Inorg. Chem.* **25,** 1481 (1986).
20. Binstead, R. A., Beattie, J. K., Dewey, T. G., and Turner, D. H., *J. Am. Chem. Soc.* **102,** 6442 (1980).
21. Binstead, R. A., Beattie, J. K., Dose, E. V., Tweedle, M. F., and Wilson, L. J., *J. Am. Chem. Soc.* **100,** 5609 (1978).
22. Birker, P. J. M. W. L., Bour, J. J., and Steggerda, J. J., *Inorg. Chem.* **12,** 1254 (1973).
23. Buhks, E., Navon, G., Bixon, M., and Jortner, J. *J. Am. Chem. Soc.* **102,** 2918 (1980).
24. Burger, K., and Ebel, H., *Inorg. Chim. Acta,* **53,** L105 (1981).
25. Caldin, E. F., and Field, J. P., *J. Chem. Soc. Faraday Trans. I* **78,** 1923 (1982).
26. Campbell, L., and McGarvey, J. J., *J. Chem. Soc. Chem. Commun.* 749 (1976).
27. Campbell, L., and McGarvey, J. J., *J. Am. Chem. Soc.* **99,** 5809 (1977).
28. Campbell, L., McGarvey, J. J., and Samman, N. G., *Inorg. Chem.* **17,** 3378 (1978).
29. Cecconi, F., Di Vaira, M., Midollini, S., Orlandini, A., and Sacconi, L., *Inorg. Chem.* **20,** 3423 (1981).
30. Chandrasekhar, K., and Bürgi, H. B., *Acta Crystallogr.* **B40,** 387 (1984).
31. Chisholm, M. H., Kober, E. M., Ironmonger, D. J., and Thornton, P., *Polyhedron* **4,** 1869 (1985).
32. Christiansen, L., Hendrickson, D. N., Toftlund, H., Wilson, S. R., and Xie, C. L., *Inorg. Chem.* **25,** 2813 (1986).
33. Coates, J. H., Hadi, D. A., Lincoln, S. F., Dodgen, H. W., and Hunt, J. P., *Inorg. Chem.* **20,** 707 (1981).
34. Cotton, F. A., Diebold, M. P., O'Connor, C. J., and Powell, G. L., *J. Am. Chem. Soc.* **107,** 7438 (1985).
35. Cox, M., Darken, J., Fitzsimmons, B. W., Smith, A. W., Larkworthy, L. F., and Rogers, K. A., *J. Chem. Soc. Dalton Trans.* 1192 (1972).
36. Crawford, T. H., and Swanson, J., *J. Chem. Educ.* **48,** 382 (1971).
37. Creutz, C., and Sutin, N., *J. Am. Chem. Soc.* **95,** 7177 (1973).
38. Cusamano, M., *J. Chem. Soc. Dalton Trans.* 2133, 2137 (1976).
39. Decurtins, S., Gütlich, P., Hasselbach, K. M., Hauser, A., and Spiering, H., *Inorg. Chem.* **24,** 2174 (1985).
40. Decurtins, S., Gütlich, P., Köhler, C. P., and Spiering, H., *J. Chem. Soc. Chem. Commun.* 430 (1985).
41. Decurtins, S., Gütlich, P., Köhler, C. P., Spiering, H., and Hauser, A., *Chem. Phys. Lett.* **105,** 1 (1984).
42. De Filippo, D., Depalano, P., Diaz, A., Steffé, S., and Trogu, E. F., *J. Chem. Soc. Dalton Trans.* 1566 (1977).
43. Dewey, T. G., and Turner, D. H., *Adv. Mol. Relax. Interact. Process.* **13,** 331 (1978).
44. DiBenedetto, J., Arkle, V., Goodwin, H. A., and Ford, P. C., *Inorg. Chem.* **24,** 455 (1985).
45. Dose, E. V., Hoselton, M. A., Sutin, N., Tweedle, M. F., and Wilson, L. J., *J. Am. Chem. Soc.* **100,** 1141 (1978).
46. Dose, E. V., Tweedle, M. F., Wilson, L. J., and Sutin, N., *J. Am. Chem. Soc.* **99,** 3886 (1977).
47. Ducommun, Y., and Merbach, A., *In* "Inorganic High Pressure Chemistry" (R. van Eldik, ed.). Elsevier, New York, 1986.
48. Dyson, H. J., and Beattie, J. K., *J. Biol. Chem.* **257,** 2267 (1982).
49. Eaton, D. R., *J. Am. Chem. Soc.* **90,** 4272 (1968).
50. Eggers, F., and Kustin, K., *In* "Methods in Enzymology" (K. Kustin, ed.), Vol. XVI, pp. 55 80. Academic Press, New York, 1969.
51. Endicott, J. F., Lessard, R. B., Lei, Y., Ryu, C. K., and Tamilarasan, R., *ACS Symp. Ser.* **307,** 85 (1986).

52. Ewald, A. H., Martin, R. L., Sinn, E., and White, A. H., *Inorg. Chem.* **8**, 1837 (1969).
53. Ewald, A. H., and Sinn, E., *Inorg. Chem.* **6**, 40 (1967).
54. Evans, D. F., *J. Chem. Soc.* 2003 (1959).
55. Evans, D. F., and James, T. A., *J. Chem. Soc. Dalton Trans.* 723 (1979).
56. Federer, W. D., and Hendrickson, D. N., *Inorg. Chem.* **23**, 3861 (1984).
57. Federer, W. D., and Hendrickson, D. N., *Inorg. Chem.* **23**, 3870 (1984).
58. Figgis, B. N., Kucharski, E. S., and White, A. H., *Aust, J. Chem.* **36**, 1537 (1983).
59. French, T. C., and Hammes, G. G., *In* "Methods in Enzymology" (K. Kustin, ed.), Vol. XVI, pp. 3 30. Academic Press, New York, 1969.
60. Godfrey, A. F., Ph.D. thesis, University of Sydney, 1985.
61. Godfrey, A. F., and Beattie, J. K., *Inorg. Chem.* **22**, 3794 (1983).
62. Goodwin, H. A., *Coord. Chem. Rev.* **18**, 293 (1976).
63. Greenaway, A. M., O'Connor, C. J., Schrock, A., and Sinn, E., *Inorg. Chem.* **18**, 2692 (1979).
64. Greenaway, A. M., and Sinn, E., *J. Am. Chem. Soc.* **100**, 8080 (1978).
65. Gütlich, P., *Struct. Bond.* **44**, 83 (1981).
66. Gütlich, P., *Adv. Chem. Ser.* **194**, 405 (1981).
67. Gütlich, P., *In* "Mössbauer Spectroscopy Applied to Inorganic Chemistry" (G. J. Long, ed.), Vol. I, Chapter XI. Plenum, New York, 1984.
68. Gütlich, P., *In* "Chemical Mössbauer Spectroscopy" (R. H. Herber, ed.), Chap. II. Plenum, New York, 1984.
69. Gütlich, P., McGarvey, B. R., and Klaüi, W., *Inorg. Chem.* **19**, 3704 (1980).
70. Halevi, E. A., and Knorr, R., *Angew. Chem. Int. Ed. Engl.* **21**, 288 (1982).
71. Hall, G. R., and Hendrickson, D. N., *Inorg. Chem.* **15**, 607 (1976).
72. Hammes, G. G., *In* "Techniques of Chemistry" (G. G. Hammes, ed.), Vol. VI, Part II, 3rd Ed, pp. 147 185. Wiley (Interscience), New York, 1974.
73. Hauser, A., *Chem. Phys. Lett.* **124**, 543 (1986).
74. Hauser, A., Gütlich, P., and Spiering, H., *Inorg. Chem.* **25**, 4245 (1986).
75. Hay, R. W., Jeragh, B., Ferguson, G., Kaitner, B., and Ruhl, B. L., *J. Chem. Soc. Dalton Trans.* 1531 (1982).
75a. Helm, L., Meier, P., Merbach, A. E., and Tregloan, P. A., *Inorg. Chim. Acta* **73**, 1 (1983).
76. Herber, R. H., *Inorg. Chem.* **26**, 173 (1987).
77. Herber, R. H., and Casson, L. M., *Inorg. Chem.* **25**, 847 (1986).
78. Hirohari, H., Ivin, K. J., McGarvey, J. J., and Wilson, J., *J. Am. Chem. Soc.* **96**, 4435 (1974).
79. Holm, R. H., Everett, G. W., and Chakravorty, A., *Prog. Inorg. Chem.* **7**, 83 (1966).
80. Holm, R. H., and O'Connor, M. J., *Prog. Inorg. Chem.* **14**, 241 (1973).
81. Hoselton, M. A., Drago, R. S., Wilson, L. J., and Sutin, N., *J. Am. Chem. Soc.* **98**, 6967 (1976).
82. Hutchinson, B., Daniels, L., Henderson, E., Neill, P., Long, G. J., and Becker, L. W., *J. Chem. Soc. Chem. Commun.* 1003 (1979).
83. Imoto, H., and Simon, A., *Inorg. Chem.* **21**, 308 (1982).
84. Ito, T., Sugimoto, M., Ito, H., Toriumi, K., Nakayama, H., Mori, W., and Sekizaki, M., *Chem. Lett.* 121 (1983).
85. Ivin, K. J., Jamison, R., and McGarvey, J. J., *J. Am. Chem. Soc.* **94**, 1763 (1972).
86. Jesson, J. P., Trofimenko, S., and Eaton, D. R., *J. Am. Chem. Soc.* **89**, 3148 (1967).
87. Joedicke, I. B., Studer, H. V., and Yoke, J. T., *Inorg. Chem.* **15**, 1352 (1976).
88. Kaplan, M. L., Bovey, F. A., and Cheng, N. H., *Anal. Chem.* **47**, 1703 (1975).
89. Katz, B. A., and Strouse, C. E., *J. Am. Chem. Soc.* **101**, 6214 (1979).
90. Katz, B. A., and Strouse, C. E., *Inorg. Chem.* **19**, 658 (1980).

91. Kennedy, B. J., Fallon, G. D., Gatehouse, B. M. K. C., and Murray, K. S., *Inorg. Chem.* **23**, 580 (1984).
92. Kilbourn, B. T., and Powell, H. M., *J. Chem. Soc. (A)* 1688 (1970).
93. König, E., and Madeja, K., *Inorg. Chem.* **6**, 48 (1967).
94. König, E., and Kremer, S., *Theor. Chim. Acta* **23**, 12 (1971).
95. König, E., Ritter, G., and Kulshreshtha, S. K., *Chem. Rev.* **85**, 219 (1985).
96. König, E., and Watson, K. J., *Chem. Phys. Lett.* **6**, 457 (1970).
97. Kremer, S., Henke, W., and Reinen, D., *Inorg. Chem.* **21**, 3013 (1982).
98. Kunze, K. R., Perry, D. L., and Wilson, L. J., *Inorg. Chem.* **16**, 594 (1977).
99. La Mar, G. N., and Sherman, E. O., *J. Am. Chem. Soc.* **92**, 2691 (1970).
100. Lawrance, G. A., and Stranks, D. R., *Inorg. Chem.* **17**, 1804 (1978).
101. Lawrance, G. A., Suvachittanont, S., Stranks, D. R., Tregloan, P. A., Gahan, L. R., and O'Connor, M. J., *J. Chem. Soc. Chem. Commun.* 757 (1979).
102. Lawthers, I., and McGarvey, J. J., *J. Am. Chem. Soc.* **106**, 4280 (1984).
103. Lazarus, M. S., Hoselton, M. A., and Chou, T. S., *Inorg. Chem.* **16**, 2549 (1977).
104. Lincoln, S. F., Hambley, T. W., Pisaniello, D. L., and Coates, J. H., *Aust. J. Chem.* **37**, 713 (1984).
105. Lockwood, G., McGarvey, J. J., and Devonshire, R., *Chem. Phys. Lett.* **86**, 127 (1982).
106. Lohr, L. L., Jr., *J. Am. Chem. Soc.* **100**, 1093 (1978).
107. Lohr, L. L., Jr., and Grimmelmann, E. K., *J. Am. Chem. Soc.* **100**, 1100 (1978).
108. Maeda, Y., Ohshio, H., and Takashima Y., *Chem. Lett.* 943 (1982).
109. Maeda, Y., Ohshio, H., Takashima Y., Mikuriya, M., and Hidaka, M., *Inorg. Chem.* **25**, 2958 (1986).
110. Maeda, Y., Tsutsumi, N., and Takashima, Y., *Chem. Phys. Lett.* **88**, 248 (1982).
111. Maeda, Y., Tsutsumi, N., and Takashima, Y., *Inorg. Chem.* **23**, 2440 (1984).
112. Martin, R. L., and White, A. H., *Trans. Metal. Chem.* **5**, 113 (1969).
113. Matsumoto, N., Ohta, S., Yoshimura, C., Ohyoshi, A., Kohata, S., Okawa, H., and Maeda, Y., *J. Chem. Soc. Dalton Trans.* 2575 (1985).
114. McGarvey, J. J., and Lawthers, I., *J. Chem. Soc. Chem. Commun.* 906 (1982).
115. McGarvey, J. J., Lawthers, I., Heremans, K., and Toftlund, H., *J. Chem. Soc. Chem. Commun.* 1575 (1984).
116. McGarvey, J. J., and Wilson, J., *J. Am. Chem. Soc.* **97**, 2531 (1975).
117. McMahon, K. J., and Beattie, J. K., unpublished observations.
118. Merbach, A. E., Moore, P., and Newman, K. E., *J. Magn. Reson.* **41**, 30 (1980).
119. Merrithew, P. B., and Rasmussen, P. G., *Inorg. Chem.* **11**, 325 (1972).
120. Moody, W. F., and Beattie, J. K., unpublished observations.
121. Mulay, L. N., and Mulay, I. L., *Anal. Chem.* **56**, 293R (1984).
122. Müller, E. W., Ensling, J., Spiering, H., and Gütlich, P. *Inorg. Chem.* **22**, 2074 (1983).
123. Nielson, R. M., Dodgen, H. W., Hunt, J. P., and Wherland, S. E., *Inorg. Chem.* **25**, 582 (1986).
124. Ohshio, H., Maeda, Y., and Takashima, Y., *Inorg. Chem.* **22**, 2684 (1983).
125. Oliver, J. D., Mullica, D. F., Hutchinson, B. B., and Milligan, W. O., *Inorg. Chem.* **19**, 165 (1980).
126. Ostfeld, D., and Cohen, I. A., *J. Chem. Educ.* **49**, 829 (1972).
127. Pell, R. J., Dodgen, H. W., and Hunt, J. P., *Inorg. Chem.* **22**, 529 (1983).
128. Petty, R. H., Dose, E. V., Tweedle, M. F., and Wilson, L. J., *Inorg. Chem.* **17**, 1064 (1978).
129. Pignolet, L. H., Horrocks, W. DeW., and Holm, R. H., *J. Am. Chem. Soc.* **92**, 1855 (1970).
130. Pignolet, L. H., and La Mar, G. N. *In* "NMR of Paramagnetic Molecules"

(G. N. LaMar, W. DeW. Horrocks, and R. H. Holm, eds.), pp. 333–369. Academic Press, New York, 1973.

131. Poganiuch, P., and Gütlich, P., *Inorg. Chem.* **26**, 455 (1987).

132. Purcell, K. F., *J. Am. Chem. Soc.* **101**, 5147 (1979).

133. Purcell, K. F., and Zapata, J. P., *J. Chem. Soc. Chem. Commun.* 497 (1978).

134. Que, L., and Pignolet, L. H., *Inorg. Chem.* **12**, 156 (1972).

135. Rablen, D. P., Dodgen, H. W., and Hunt, J. P., *Inorg. Chem.* **15**, 931 (1976).

136. Rao, P. S., Reuveni, A., McGarvey, B. R., Ganguli, P., and Gütlich, P., *Inorg. Chem.* **20**, 204 (1981).

137. Reeder, K. A., Dose, E. V., and Wilson, L. J., *Inorg. Chem.* **17**, 1071 (1978).

138. Sachinidis, J., and Grant, M. W., *J. Chem. Soc. Chem. Commun.* 157 (1978).

139. Schmidt, J. G., Brey, W. S., and Stoufer, R. C., *Inorg. Chem.* **6**, 268 (1967).

140. Schumann, M., and Elias, H., *Inorg. Chem.* **24**, 3187 (1985).

141. Simmons, M. G., and Wilson, L. J., *Inorg. Chem.* **16**, 126 (1977).

142. Simon, A., Schnering, H. G., and Schäfer, H., *Z. Anorg. Allg. Chem.* **355**, 295 (1967).

142a. Sim, P. G., and Sinn, E., *J. Am. Chem. Soc.* **103**, 241 (1981).

143. Sinn, E., Sim, G., Dose, E. V., Tweedle, M. F., and Wilson, L. J., *J. Am. Chem. Soc.* **100**, 3375 (1978).

144. Sorai, M., *J. Inorg. Nucl. Chem.* **40**, 1031 (1978).

145. Sorai, M., and Seki, S., *J. Phys. Chem. Solids* **35**, 555 (1974).

146. Stengle, T. R., and Langford, C. H., *Coord. Chem. Rev.* **2**, 349 (1967).

147. Stuehr, J., *In* "Techniques of Chemistry" (G.G. Hammes, ed.), Vol. VI, Part II, 3rd Ed, pp. 237–283. Wiley (Interscience), New York, 1974.

148. Swift, T. J., and Connick, R. E., *J. Chem. Phys.* **37**, 307 (1962).

149. Swift, T. J., *In* "NMR of Paramagnetic Molecules" (G. N. LaMar, G. N., W. DeW. Horrocks, and R. H. Holm, eds.), pp. 53–83. Academic Press, New York, 1973.

150. Switzer, M. E., Wang, R., Rettig, M. F., and Maki, A. H., *J. Am. Chem. Soc.* **96**, 7669 (1974).

151. Takemoto, J. H., and Hutchinson, B., *Inorg. Chem.* **12**, 705 (1973).

152. Thuéry, P. and Zarembowitch, J., *Inorg. Chem.* **25**, 2001 (1986).

153. Timken, M. D., Abdel-Mawgoud, A. M., and Hendrickson, D. N., *Inorg. Chem.* **25**, 160 (1986).

154. Timken, M. D., Hendrickson, D. N., and Sinn, E., *Inorg. Chem.* **24**, 3947 (1985).

155. Timken, M. D., Strouse, C. E., Soltis, S. M., Daverio, S. A., Hendrickson, D. N., Abdel-Mawgoud, A. M., and Wilson, S. R., *J. Am. Chem. Soc.* **108**, 395 (1986).

156. Tricker, M. J., *J. Inorg. Nucl. Chem.* **36**, 1543 (1974).

157. Turner, D. H., Flynn, G. W., Sutin, N., and Beitz, J. V., *J. Am. Chem. Soc.* **94**, 1554 (1972).

158. van Geet, A. L., *Anal. Chem.* **42**, 679 (1970).

159. Vos, G., De Graaff, R. A. G., Haasnoot, J. G., Van Der Kraan, A. M., De Vaal, P., and Reedijk, J., *Inorg. Chem.* **23**, 2905 (1984).

160. Wells, F. V., McCann, S. W., Wickman, H. H., Kessel, S. L., Hendrickson, D. N., and Feltham, R. D., *Inorg. Chem.* **21**, 2306 (1982).

161. Whitesides, T. H., *J. Am. Chem. Soc.* **91**, 2395 (1969).

162. Wilkins, R. G., Yelin, R., Margerum, D. W., and Weatherburn, D. C., *J. Am. Chem. Soc.* **91**, 4326 (1969).

163. Williams, D. L., Smith, D. W., and Stoufer, R. C., *Inorg. Chem.* **6**, 590 (1967).

164. Zarembowitch, J., Claude, R., and Thuéry, P., *Nouv. J. Chim.* **9**, 467 (1985).

165. Zarembowitch, J., and Kahn, O., *Inorg. Chem.* **23**, 589 (1984).